El Sayed *et al.*
Future Journal of Pharmaceutical Sciences (2026) 12:60
https://doi.org/10.1186/s43094-026-00987-8

Future Journal of Pharmaceutical Sciences

RESEARCH Open Access

In silico and in vivo targeting of Wnt/β-catenin/GSK-3β and redox pathways: geraniol–CoQ10 as a novel cardioprotective duo against I/R injury

Nermein F. El Sayed[1*], Azza Sayed Mohamed Awad[2], Iten M. Fawzy[3], Hesham Mohamed Mahmoud[4] and Hanan S. El-Abhar[5*]

Abstract

Background Although statins confer cardioprotection via HMG-CoA reductase inhibition, they are also known to reduce CoQ10 biosynthesis. In light of previous reports suggesting that geraniol, a natural monoterpene with pleiotropic cardioprotective effects, may intersect with the mevalonate pathway, we hypothesized that combining geraniol with CoQ10 could yield enhanced cardioprotective benefits. Using in silico analyses and a rat model of myocardial ischemia/reperfusion (I/R) injury (30-min LAD occlusion followed by 120-min reperfusion with continuous ECG monitoring), we evaluated geraniol alone and with CoQ10. Male Wistar rats were allocated into five groups: sham, I/R, geraniol + I/R, CoQ10 + I/R, and geraniol + CoQ10 + I/R.

Results Preconditioning with geraniol and/or CoQ10 significantly decreased infarct size relative to the area at risk, preserved myocardial histoarchitecture, and mitigated cardiac biomarkers (CK-MB, LDH, cTn-I) and ST-segment elevation. Molecularly, treatments suppressed GSK-3β, a pivotal mediator of I/R injury, via activation of the Wnt/β-catenin pathway, while reinforcing antioxidant defenses (SOD, GSH) and reducing lipid peroxidation. They also inhibited inflammatory mediators (pSer536-NF-κB, TNF-α), neutrophilic infiltration (ICAM-1, MPO), curtailed caspase-3, and elevated Bcl-2, reflecting strong anti-inflammatory and antiapoptotic actions. In silico docking also predicted the ability of geraniol and CoQ10 to interact with GSK-3β and NF-κB. Notably, the combination therapy conferred the greatest protection.

Conclusion Overall, these findings identify geraniol and CoQ10, particularly in combination, as promising cardioprotective agents against I/R injury through modulation of Wnt/GSK-3β/β-catenin signaling and associated antioxidative, anti-inflammatory, and antiapoptotic pathways.

Article Highlights

(1) Geraniol and CoQ10 guard against I/R injury.
(2) Combination therapy outperforms single treatments.

*Correspondence:
Nermein F. El Sayed
Nermein.fawzy@acu.edu.eg
Hanan S. El-Abhar
hanan.elabhar@fue.edu.eg
Full list of author information is available at the end of the article

(3) Limits infarct size, preserves heart structure & ECG.
(4) Wnt activation with GSK-3β inhibition orchestrate protection.
(5) Treatments enhance antioxidant, anti-inflammatory, anti-apoptotic defense.

Keywords Myocardial ischemia/reperfusion, Geraniol, Coenzyme Q10, GSK-3β, β-catenin, Anti-inflammatory, Antioxidant

Introduction

Despite advances in prevention and treatment, coronary heart disease, including acute myocardial infarction (AMI), remains a leading cause of death and disability worldwide, with incidence and outcomes varying by age, sex, and geographic region [1]. Recent epidemiological data indicate that AMI incidence has risen over the past decade, peaking in 2021, with a modest decline by 2024. ST-elevated myocardial infarction (STEMI) comprised over half of cases, predominantly affecting younger men, whereas non-STEMI (NSTEMI) was more common among older patients with comorbidities [2]. Hypertension, smoking, diabetes, and dyslipidemia were the most prevalent risk factors [3]. AMI occurs when coronary blood flow is abruptly reduced, depriving cardiac tissue of oxygen and triggering ischemic injury, and while this reduction is often multifactorial, it is most commonly initiated by rupture or erosion of an atherosclerotic plaque, leading to platelet activation, thrombus formation, and subsequent myocardial ischemia and necrosis [3, 4].

AMI precipitates ischemia-driven cellular injury [5], a phenomenon that transpires during various cardiac interventions [6]. Paradoxically, reperfusion therapy, essential for salvaging myocardium, can exacerbate damage through ischemia/reperfusion (I/R) injury [5, 6]. Myocardial I/R pathobiology involves disrupted bioenergetics, neutrophilic infiltration, and excessive formation of reactive oxygen species (ROS) [7] that flares upon reperfusion [8], impairing cardiomyocytes and endothelial cells while instigating inflammatory cascades [9]. Thwarting I/R injury is, therefore, pivotal for mitigating ischemic cardiac conditions [7].

The Wnt/Frizzled signaling pathway is a complex network essential for various vital processes [10], with glycogen synthase kinase-3β (GSK-3β), a key regulator within this cascade [5]. Wnt signaling activation causes GSK-3β inactivation to stabilize β-catenin, which acts as a transcription factor [11] along with alleviating apoptosis by inducing B-cell lymphoma 2 (Bcl-2) [12]. A previous study in the cardiovascular system indicated that β-catenin signaling mediates protection against I/R injury through its antiapoptotic effects [13]. While early studies largely focused on chronic heart failure and post-infarction remodeling, accumulating evidence highlights a pivotal role for GSK-3β dysregulation in AMI. GSK-3β has been implicated in the pathogenesis of AMI, influencing cardiomyocyte survival, apoptosis, and inflammatory responses [14]. Both preclinical and clinical data indicate that aberrant activation of GSK-3β during I/R contributes to infarct expansion, adverse remodeling, and impaired cardiac function. In fact, modulation of GSK-3β activity intersects with key signaling cascades, including abrogation of nuclear factor kappa B (NF-κB), a central orchestrator of inflammation [5, 15], to underscore its cardioprotective role [16] during I/R, positioning it as a promising therapeutic target to mitigate AMI and enhance cardioprotection [14].

To attenuate I/R insult, pharmacological compounds targeting distinct signaling cascades have demonstrated notable efficacy. Beyond conventional pharmacotherapies, nutraceuticals offer a broad safety margin and serve as a preventive strategy to shield the myocardium. Remarkably, statins confer cardioprotection primarily by inhibiting 3-hydroxy-3-methylglutaryl coenzyme A (HMG-CoA) reductase enzyme. Interestingly, geraniol, a naturally occurring monoterpene alcohol found in rose, palmarosa, and various essential oils, has been reported in several studies to modulate the mevalonate pathway, potentially acting on HMG-CoA reductase [17, 18]. Geraniol exhibits multiple pharmacological benefits, including antioxidant, anti-inflammatory, antimicrobial, and antiapoptotic properties, and has demonstrated cardioprotective effects against various cardiac stressors [19]. Notably, inhibition of the mevalonate pathway can reduce coenzyme Q10 (CoQ10) levels in plasma and platelets, which are often already deficient in cardiomyopathy patients [20, 21]. Aside from being essential for mitochondrial oxidative phosphorylation, particularly in energy-demanding cells like cardiomyocytes [22], CoQ10 has redox-modulating prowess, constituting the cornerstone of its myocardial safeguarding potential [23].

Given that curbing HMG-CoA reductase activity may exhaust this vital bioenergetic cofactor, the present study sought to decipher the mechanistic underpinnings of geraniol's cardioprotective efficacy, alone and in combination with CoQ10, against myocardial I/R affront. This approach allows investigation of complementary mechanisms of protection, including antioxidant,

anti-inflammatory, and antiapoptotic effects, while clarifying their potential synergistic impact on cardiac resilience.

Materials and methods

Animals

This study adheres to the ARRIVE guidelines and the *Guide for the Care and Use of Laboratory Animals* issued by the US National Institutes of Health (NIH Publication No. 85-23, revised 1996). The study was conducted on 48 healthy adult male Wistar rats purchased from the National Research Centre, Giza, Egypt, each weighing between 250 and 300 g. The rodents were hosted under stable environmental settings, maintaining regulated temperature and humidity levels, alongside a balanced light/dark cycle, for one week preceding the experimental procedures. They were granted unrestricted access to a standard commercial rat pellet diet and potable water.

Induction of I/R

Anesthetized rodents (administered ketamine (100 mg/kg)/xylazine (10 mg/kg); intraperitoneally) [24] underwent endotracheal intubation for facilitated mechanical ventilation. To mitigate the onset of hypothermia, a heating lamp was utilized, with body temperature closely monitored using a thermometer. Subcutaneous peripheral limb electrodes were positioned, enabling continuous electrocardiographic (ECG) surveillance throughout the experimental period via a polygraph (Letica polygraph 4006, Spain). A dermal incision was executed along the left clavicular midline, followed by meticulous blunt muscle separation. After thoracotomy, the pericardium was incised, and the left anterior descending (LAD) coronary artery was ligated. Successful ischemic modeling was confirmed upon the manifestation of ST-segment elevation within 2 min. After a 30-min occlusion, the clamp was disengaged, reinstating perfusion for a subsequent 120-min period [25].

Experimental design

Rodents were randomly allocated into five cohorts using a simple randomization sequence generated in Microsoft Excel, followed by sorting and sequential allocation into experimental groups. In the initial cohort (n = 8), animals underwent all surgical procedures except for coronary artery ligation, serving as the sham-operated control group. The remaining 40 rodents were apportioned into four subsets (n = 10 each). In the second group, animals were subjected to left anterior descending (LAD) coronary artery I/R to establish the untreated injury model. Subjects in groups 3, 4, and 5 were administered geraniol (Ger, 100 mg/kg [26, 27]; Sigma-Aldrich Chemicals, MO, USA), coenzyme Q10 (CoQ10, 200 mg/kg [28, 29]; MEPACO Pharmaceutical Company, Cairo, Egypt), or their concomitant regimen, respectively. The designated compounds were orally gavaged for seven consecutive days, and on the eighth day, all rodents in the latter three cohorts underwent the I/R surgical procedure (Fig. 1).

Assessment of ECG

ECG recordings were obtained prior to ischemia induction to establish a baseline ECG pattern, which served as the standard reference for each rat. Thereafter, ECG tracings were continuously monitored throughout the 2-h experimental timeline encompassing ischemia and reperfusion [30, 31]. The analysis of ST-segment elevation was specifically conducted using lead II as commonly employed in experimental myocardial I/R models [32]. All ECG analyses were conducted by investigators blinded to the experimental group allocation to minimize assessment bias.

Assessment of area at risk and myocardial infarction size

Area at risk (AAR) using methylene blue

In the four cohorts subjected to I/R, two representative rodents per group were selected for the evaluation of the AAR. Following reperfusion and immediately prior to euthanasia, the left coronary artery was re-occluded, and 0.6 ml of 1% methylene blue dye (Sigma Chemical Co.) was injected into the left ventricle to delineate the AAR, which was identified by visually tracing the unstained region [33]. Subsequently, the heart was excised, enveloped in paraffin film to prevent desiccation, and frozen for 60 min at – 20 °C. The ventricles designated for staining were sectioned transversely into four slices (2 mm thick) from the apex to the occlusion site, and the AAR was quantified as the region devoid of blue staining. Each section was digitally captured using a high-resolution camera, and planimetric assessment of the pale regions was performed utilizing ImageJ® software. The AAR was then computed as a percentage of the total ventricular area for each slice.

Infarct area using TTC stain

The previous methylene blue slices were re-used to clarify the actual infarcted area relative to the injured one using the TTC dye (Sigma-Aldrich Co.) that was added to the slices to distinguish viable tissue from the necrotic tissue [34]**.** The TTC stain can quantify the necrotic area reliably within "3—6 h" after coronary occlusion, even before histologic changes can be diagnosed [35]. Therefore, the slices were soaked in TTC and incubated in the dark for 20 min at room temperature. At the end of the incubation period, the color of the viable tissue turns deep red (tri-phenyltetrazolium), while the pale area indicates the infarcted non-viable tissue. Once the color

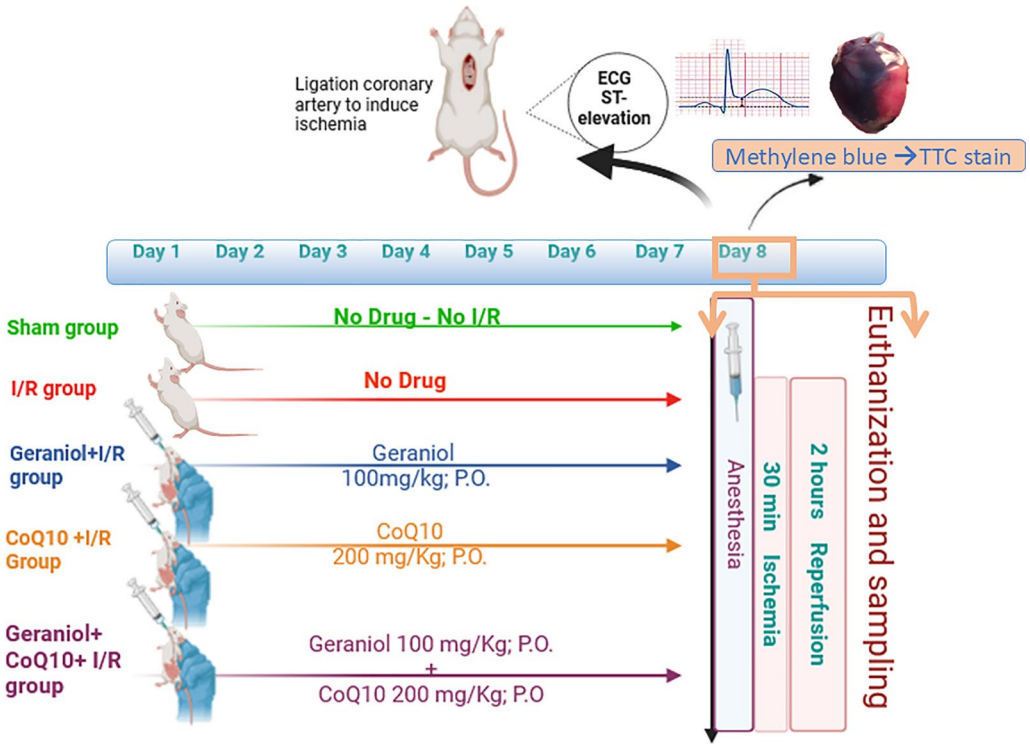

Fig. 1 Schematic representation of the experimental design illustrating five groups: sham, I/R, and three cohorts preconditioned with geraniol, CoQ10, or their combination for seven consecutive days. I/R injury was induced on day 8 (30 min/2 h). ECG recordings were obtained, blood samples were collected, and heart tissues were harvested post-euthanization

has been established, the slices were fixed in 10% formalin for another 20 min to increase the contrast [36]. The infarct size was determined by measuring the area of infarction in a series of slices, and the average was calculated to be presented as the infarct area. The percentage of infarct area to AAR (infarct area/AAR)% was calculated by dividing the calculated infarct area by the AAR and multiplied by 100 [37].

Preparation of samples

Following 120 min of reperfusion, aortic blood was drawn to isolate sera, which were portioned and preserved at – 80 °C for subsequent assessment of serum biomarkers. Thereafter, the hearts from six specimens per cohort were swiftly harvested, rinsed with chilled saline, weighed, and homogenized in ice-cold saline to yield a 10% tissue homogenate [38].

Assessment of biochemical markers:

Assessment of serum myocardial cellular injury biomarkers

The corresponding ELISA colorimetric kits, purchased from Kamiya Biomedical Company (WA, USA), were used to measure the serum levels of lactate dehydrogenase (LDH; cat # KT-20242), while that of cardiac troponin I (cTn-I; cat. # MBS727624) was supplied from MyBioSource, Inc (CA, USA), and creatine kinase–MB isoenzyme (CK-MB; cat # E0311Ra) was supplied from Shanghai Crystal-day Biotech Co. (Shanghai, China); all instructions were followed according to the manufacturer.

Measurement of redox parameters

The cardiac content of malondialdehyde (MDA), a marker for lipid peroxidation, was determined using the TBARS Assay Kit (Oxiselect™, San Diego, CA, USA; cat. # STA-330), while the corresponding kits for reduced glutathione (GSH; cat. # GR 2511) and superoxide dismutase (SOD; cat. # SD 2521) were procured from Biodiagnostic Co. (Cairo, Egypt). Tissue protein was determined according to Bradford's method using the corresponding kit (Protein Assay Kit (SK3041; Bio Basic, ON, Canada)).

Assessment of inflammatory markers

The myocardial concentrations of phosphorylated (S536)-NF-κB (MyBioSource, Inc., CA, USA; cat. # MBS846727) and tumor necrosis factor (TNF)-α (Ray-Biotech, GA, USA; cat. # ELR-TNFalpha-001C) were

quantified utilizing ELISA assay kits, adhering strictly to the protocols delineated by the respective manufacturers.

Measurement of neutrophil infiltration parameters

The homogenate was employed for the quantification of intercellular adhesion molecule-1 (ICAM-1) contents using the respective ELISA assay kit (EIAab Co., Wuhan, China; cat. # E0048r). Moreover, the chromogenic assay method of Krawisz et al. [39] was implemented to evaluate the enzymatic activity of myeloperoxidase (MPO), wherein one enzymatic unit was characterized as the amount catalyzing the degradation of 1 µmol of peroxide per minute.

Assessment of GSK-3β /β-catenin pathway and the antiapoptotic marker Bcl-2

The ELISA assay kits were procured from MyBioSource, to quantify the myocardial contents of GSK-3β (cat. # MBS766198) and β-catenin (non-phospho active, cat. # MBS7269476), and from Cusabio (Wuhan, China) for the antiapoptotic biomarker Bcl-2 (cat. # CSB-E08854r). The experimental procedures for all utilized kits were meticulously executed in strict accordance with the manufacturer's guidelines.

Histological examination

The hearts from two representative animals per group [40] were carefully excised in their entirety and meticulously dissected to remove any adhering connective tissue and major blood vessels. Immediately following extraction, the hearts were immersed in a fixative solution comprising 10% formalin saline to preserve tissue integrity and prevent autolysis. After fixation, the specimens were dehydrated through a graded series of ethanol solutions, cleared in xylene, and subsequently embedded in paraffin to facilitate sectioning. Thin tissue sections were then cut using a microtome, mounted onto glass slides, and stained with hematoxylin and eosin (H&E) to highlight cellular and structural details. The prepared slides were examined under a light microscope to assess histopathological changes associated with I/R injury and the effects of the administered treatments.

Immunohistopathology assay

Paraffin-embedded cardiac tissue sections were mounted on positively charged slides by using avidinbiotin–peroxidase complex (ABC) method. Sections from each group were then incubated with these primary antibodies targeting caspase-3 (ABclonal; cat. # A11953; USA); then, the reagents required for ABC method were added (Vectastain ABC-HRP kit, Vector laboratories). Marker expression was labeled with peroxidase and colored with diaminobenzidine (DAB, produced by Sigma) to detect antigen–antibody complex. Negative controls were included using non-immune serum in place of the primary or secondary antibodies. IHC stained sections were examined using an Olympus microscope (BX-63).

Quantitative analysis of staining was conducted by determination of reaction area percentage in 7 microscopic fields using ImageJ 1.53t, Wayne Rasband and contributors, National Institutes of Health, USA.

AAR and infarct size measurements, histopathological changes, and immunohistochemical analysis were performed by a pathologist blinded to experimental group allocation.

Molecular docking

A virtual molecular docking study was performed using Discovery Studio 4.0 to investigate the potential mechanisms of action of geraniol and CoQ10 against glycogen synthase kinase-3 beta (GSK-3β) and nuclear factor kappa B (NF-κB). The three-dimensional structures of geraniol and CoQ10 were retrieved from the PubChem database in SD file format. The ligands were prepared by applying the CHARMm force field and MMFF partial charges, followed by energy minimization.

The crystal structure of GSK-3β complexed with an inhibitor [41] (PDB ID: 4ACD) was obtained from the Protein Data Bank. The protein structure was examined for missing residues and corrected accordingly, hydrogen atoms were added, and the same force field was applied. Energy minimization was performed using the Adopted Basis Newton–Raphson (NR) algorithm for 2000 steps. The active site of the receptor was defined based on the binding region of the co-crystallized reference inhibitor, 3-amino-6-{4-[(4-methylpiperazin-1-yl)sulfonyl]phenyl}-N-pyridin-3-ylpyrazine-2-carboxamide (GR9). Subsequently, the C-Docker protocol was utilized to dock the reference inhibitor, geraniol, and CoQ10 into the active site of GSK-3β. For each ligand, ten distinct binding conformations were generated along with their corresponding C-Docker interaction energies) in Kcal/mol. Docking validation was obtained via redocking of the complexed inhibitor (GR9) from protein data bank, and ligand alignment was performed where generated RMSD was 1.03 Å.

Similarly, the crystal structure of human NF-κB p52 bound to DNA [42] (PDB ID: 1A3Q) was retrieved and prepared using the same procedure. The potential binding site was identified from the reported inhibitory cavities within the structure. Geraniol and CoQ10 were then docked into the NF-κB binding site using the C-Docker protocol.

Molecular dynamic simulations were conducted in Discovery Studio 4.0 using a combination of the Steepest

Descent and Conjugate Gradient algorithms for energy minimization over 1000 steps. The simulations were carried out in three phases, namely heating, equilibration, and production over a temperature range of 50–300 K and for a total simulation time of 200 ns under an number of particles, volume, and temperature (NVT) ensemble, employing a leap-frog integrator with a time step of 1,000 and explicit solvent model BMSW (Boltzmann–Simple Switching) [43]. The resulting trajectories were analyzed to determine total energy (kcal/mol) as a function of time (ns), as well as van der Waals and hydrogen bonding energies. Additionally, root-mean-square deviation (RMSD) and root-mean-square fluctuation (RMSF) analyses were performed to evaluate conformational stability and residue flexibility.

Statistical analysis

Based on data obtained from 6 to 8 animals per group, all values are expressed as the mean ± SD. For all the assessed values, homoscedasticity test was conducted using Bartlett's test. Statistical analyses were conducted using a one-way analysis of variance (ANOVA) to assess differences among groups, followed by Tukey's post hoc test for multiple comparisons. For the parameters where the assumption of homogeneity of variances is violated, the Welch's ANOVA test is used followed by Games-Howell's multiple comparison test. A probability value (P) of less than 0.05 was considered statistically significant. Pearson's correlation coefficient was calculated to assess the correlation between GSK-3β and β-catenin, between GSK-3β and the rest of the markers, and between β-catenin and NF-κB. All statistical procedures and representations of the data were generated using GraphPad Prism version 8.0.

Results

Geraniol and/or CoQ10 attenuate ST-segment elevation following myocardial I/R affront

As illustrated in Fig. 2, panel (A) shows electrocardiographic (ECG) recordings, while panel (B) quantifies ST-segment elevation during ischemia. At the onset of ischemia, a modest yet significant increase in the ST segment was detected relative to the sham group. This elevation progressed throughout the ischemic phase, reaching approximately 1.7-fold of sham values.

Panel (C) demonstrates the reperfusion phase, where ST-segment elevation further intensified upon reperfusion initiation and remained significantly elevated at the end of the reperfusion period. Pre-treatment with geraniol, CoQ10, or their combination mitigated these alterations, with the combined regimen restoring ST-segment values closest to baseline.

Geraniol and/or CoQ10 reduce myocardial infarct size

Myocardial I/R injury produced a marked infarct size reaching 66.23% of the area at risk (AAR). Preconditioning with geraniol, CoQ10, or their combination significantly limited infarct expansion, with the combined regimen exerting the most pronounced cardioprotective effect (Fig. 3A–C**).**

Geraniol and/or CoQ10 suppress myocardial injury biomarkers

As shown in Fig. 4, I/R injury induced a substantial rise in cardiac biomarkers, including **(A)** CK-MB, (B) cTn-I, and (C) LDH, which increased by approximately 4-, 6.6-, and 3.9-fold, respectively, compared to sham. Pre-treatment with geraniol and/or CoQ10, however, significantly blunted these elevations. Notably, geraniol alone and in combination with CoQ10 nearly normalized these biomarkers, indicating robust cardioprotection.

Geraniol and/or CoQ10 preserve myocardial histoarchitecture

As depicted in Fig. 5**,** representative myocardial histology sections reveal that (A, B) control groups exhibited intact cardiac architecture with well-organized fibers, clear striations, and absence of inflammatory infiltration. In contrast, (C, D) I/R injury resulted in severe structural disruption, including vascular congestion [V], inflammatory cell infiltration [M], and myocardial degeneration [D]. Pre-treatment with (E, F) geraniol or (G, H) CoQ10 markedly attenuated these alterations, while (I, J) their combination conferred superior preservation of myocardial structure [My].

Geraniol and/or CoQ10 modulate the cardiac GSK-3β/β-catenin/Bcl-2 /caspase-3 trajectory in rats subjected to I/R injury

Induction of I/R injury (Fig. 6) significantly activated pro-apoptotic signaling, evidenced by a sixfold increase in myocardial GSK-3β, accompanied by marked reductions in β-catenin and Bcl-2 levels by 75% and 84%, respectively. Pre-treatment with geraniol, CoQ10, or their combination significantly reversed these alterations, with the combination almost completely restoring axis homeostasis. Similarly, immunohistochemical analysis (Fig. 7) revealed a dramatic increase in caspase-3 expression (63-fold) in the I/R group. However, all treatments significantly reduced caspase-3 expression, with the combination exerting the most pronounced suppression reaching 95% decrease in caspase-3 expression.

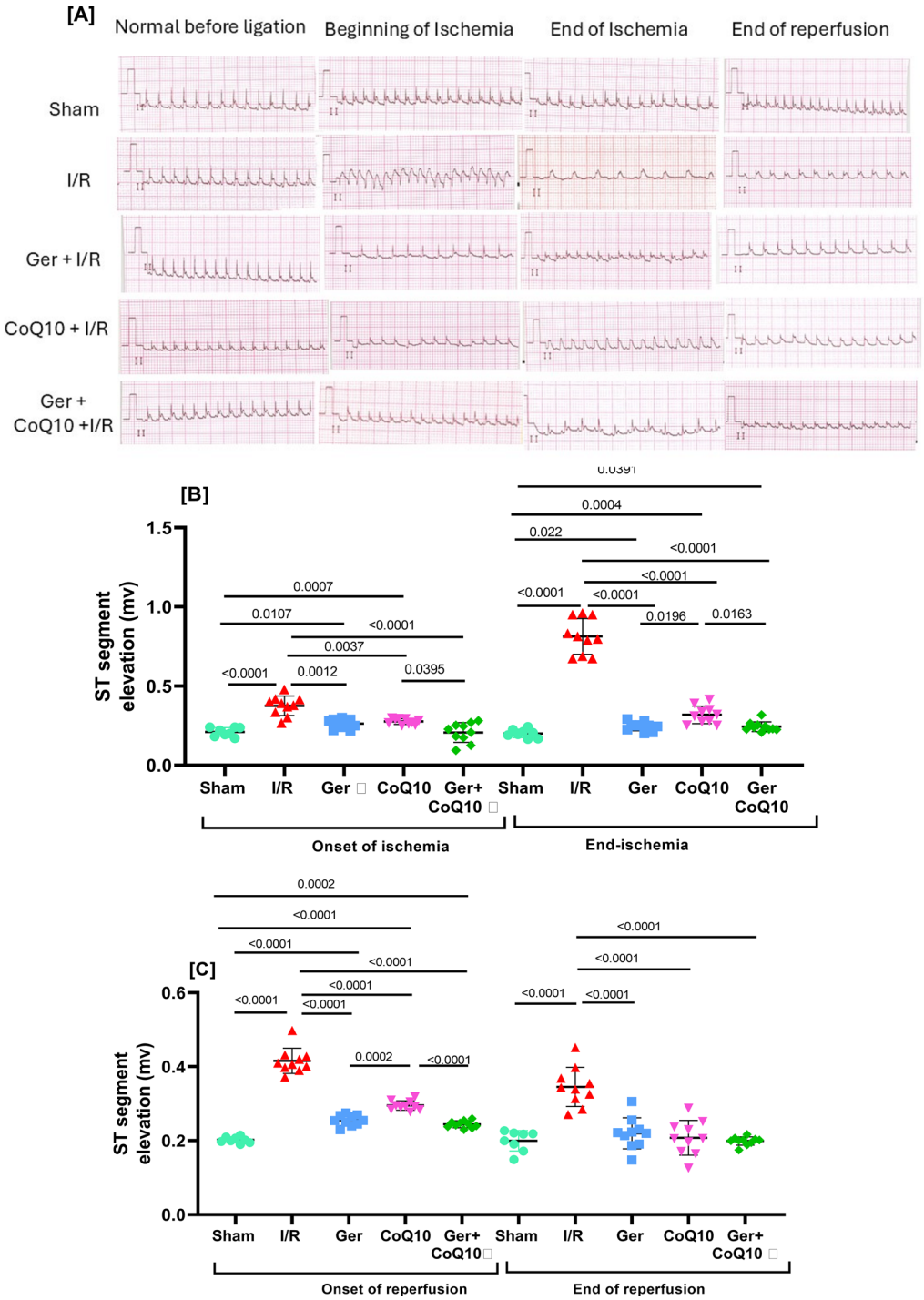

Fig. 2 Effect of preconditioning with geraniol and/or CoQ10 regimens on ST-segment elevation. **A** Representative ECG records, **B** onset and end of the ischemic phase, and **C** onset and end of the reperfusion phase. Data of 6–8 animals were presented as mean ± SD. Welch's ANOVA (ischemia) followed by Games-Howell's multiple comparison test and one-way ANOVA followed by Tukey's post hoc test (reperfusion) were adopted to assess significant differences. A probability value (P) of less than 0.05 was considered statistically significant

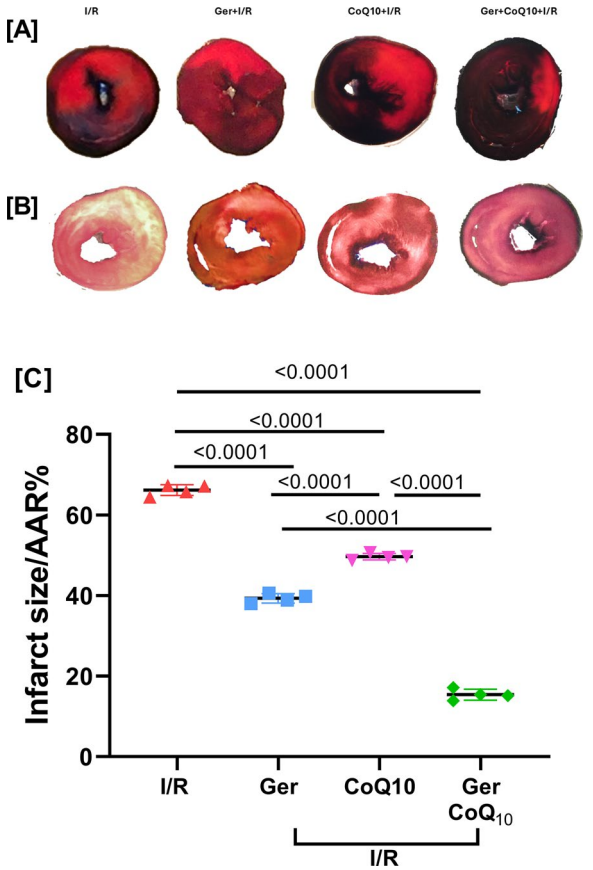

Fig. 3 Effect of geraniol and/or CoQ10 on **A** the area at risk (AAR), **B** infarcted area, and **C** percent of infarcted area to AAR using methylene blue and TTC, respectively, in rats subjected to I/R injury (n = 2, each of 4 sections). The AAR was defined as regions not stained with blue dye, shown in the upper panels, and the infarct area was defined as regions not stained with TTC (white area), shown in the lower panels. The infarct size, or the percent infarct area, was evaluated as a percentage of the infarct area relative to the area at risk. Data of 8 observations were presented as mean ± SD. One-way ANOVA followed by Tukey's post hoc test was adopted to assess significant differences. A probability value (P) of less than 0.05 was considered statistically significant. AAR: area at risk; TTC: 2,3,5-triphenyltetrazolium chloride

Geraniol and/or CoQ10 restore redox balance in rats subjected to I/R injury

As shown in Fig. 8, I/R injury induced severe oxidative duress, reflected by a 389% increase in (A) MDA levels, alongside depletion of the defense molecules (B) GSH and (C) SOD. Treatment with geraniol and/or CoQ10, on the other hand, restored antioxidant defenses and reduced lipid peroxidation, with the combined regimen demonstrating superior efficacy.

Combined geraniol and CoQ10 regimen mitigate myocardial inflammatory markers in rats subjected to I/R injury

Figure 9 shows that I/R injury *triggered a robust inflammatory response,* evidenced by about fivefold elevations in the transcriptional regulator (A) p(S536)-NF-κB and (B) TNF-α. This upsurge extended to cause around 4.5-fold elevation in the neutrophil infiltration-related markers (C) ICAM-1 and (D) MPO. All treatments significantly attenuated these inflammatory mediators, with the combination therapy restoring several parameters to near-sham levels. Notably, geraniol exhibited stronger effects on ICAM-1 normalization, whereas CoQ10 produced partial attenuation.

Correlation analysis between GSK and assessed parameters

Pearson's correlation analysis revealed strong associations between GSK-3β and multiple pathological markers, as well as β-catenin and NF-κB. As shown in Fig. 10, GSK-3β showed strong positive correlations ($P < 0.0001$) with injury, oxidative, and inflammatory markers and strong negative correlations with antioxidant and antiapoptotic indices. Conversely, β-catenin negatively correlated with NF-κB, reinforcing the interconnected regulatory role of this signaling axis.

Geraniol and CoQ10 possible inhibition of GSK3β and NF-κB

Since activated GSK-3β is strongly implicated in the pathogenesis of cardiac disorders and promotes NF-κB activation, thereby sustaining pro-inflammatory signaling, both GSK-3β and NF-κB represent interconnected therapeutic targets. This rationale guided their selection in the present in silico study to explore the potential inhibitory mechanisms of geraniol and to compare its activity with CoQ10.

Molecular docking was then performed to assess the inhibitory potential of geraniol and CoQ10 against GSK-3β relative to the co-crystallized reference ligand (GR9). As illustrated in Fig. 11, the reference complex formed hydrogen–bond interactions with key residues Arg148, Arg144, Tyr140, Glu249, Ala143, and Glu253, exhibiting a—(C-docker interaction energy) of -19.56 kcal/mol. In comparison, geraniol demonstrated comparable binding behavior, forming hydrogen bonds with the critical residues Arg148 and Tyr140, with a—(C-docker interaction energy) of -10.69 kcal/mol and RMSD of 2.03 Å in ligand validation overlay study. In contrast, CoQ10 displayed a—(C-docker interaction energy) of − 39.21 kcal/mol but interacted with non-essential residues, including Ser215, Tyr216, and Ile228 through hydrogen

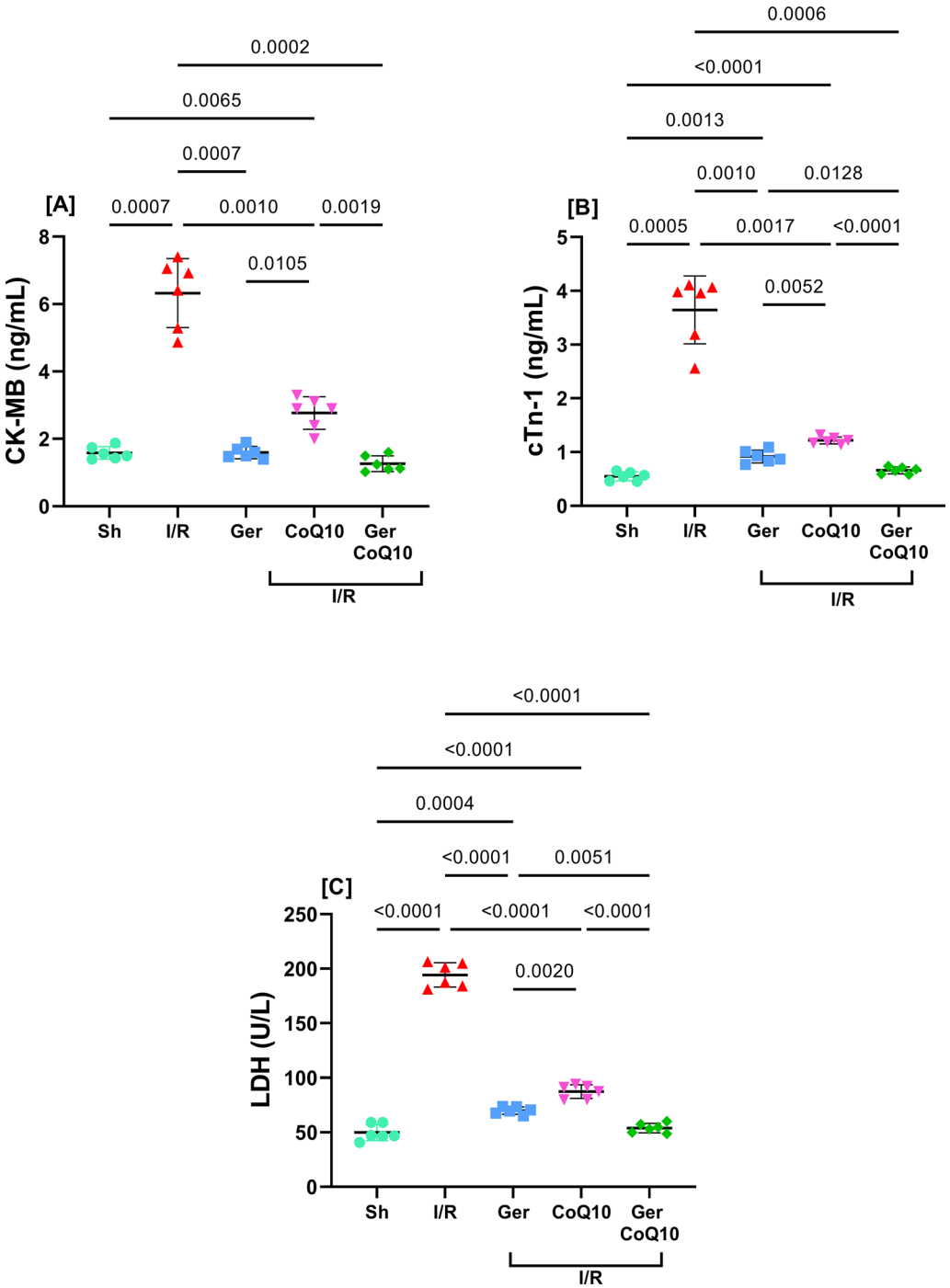

Fig. 4 Effect of preconditioning with geraniol and/or CoQ10 regimens on **A** CK-MB, **B** cTn-I, and **C** LDH in myocardial I/R affront in rats. Data of 6 observations were presented as mean ± SD. Welch's ANOVA test followed by Games-Howell's multiple comparison test (CK-MB, cTn-I) and one-way ANOVA followed by Tukey's post hoc test (LDH) were adopted to assess significant differences. A probability value (P) of less than 0.05 was considered statistically significant. CoQ10: coenzyme Q10; CK-MB: creatine kinase–MB isoenzyme; cTn-I: cardiac troponin-I; LDH: lactate dehydrogenase

bonding, as well as π-interaction with Arg228, located away from the active binding site.

Subsequent docking studies against NF-κB revealed that geraniol was successfully accommodated within the inhibitory cavity (A1/A2 pockets) (Fig. 12) compared to

key interacting residues reported in the literature [44], exhibiting an interaction energy of − 25.99 kcal/mol and forming hydrogen bonds with His105 and Lys153, similar to the literature study on natural compounds, along with π-interactions involving Ala104 and Ile119. Conversely, CoQ10 failed to occupy the inhibitory binding pocket of NF-κB.

These docking findings were further validated by molecular dynamics simulation studies performed on both the free and geraniol-bound forms of GSK3β and NF-κB over a 200-ns simulation period. The total energy of free GSK-3β ranged from − 10,590 to − 10,806 kcal/mol, while the geraniol-bound complex exhibited a comparable and stable range of − 10,610 to − 10,732 kcal/mol (Fig. 13). Similarly, free NF-κB displayed total energy values between − 9693 and − 9783 kcal/mol, whereas the geraniol-bound system maintained a stable energy profile.

Analysis of hydrogen bonding further supported the enhanced stability of the geraniol–protein complexes. Free GSK-3β exhibited hydrogen bonding energies between − 2397 and − 2524 kcal/mol, which slightly increased upon geraniol binding (− 2378 to − 2535 kcal/mol), indicating additional stabilizing interactions. Likewise, the hydrogen bonding energy of free NF-κB (− 1829 to − 1933 kcal/mol) increased in the presence of geraniol (− 1848 to − 1975 kcal/mol).

As depicted in Fig. 14A, trajectory analysis demonstrated that the root-mean-square deviation (RMSD) of free GSK-3β ranged from 1.55 to 3.34 Å, while the geraniol-bound complex fluctuated between 1.12 and 10.29 Å, with minor deviations observed in the later stages of the simulation. For NF-κB, the RMSD of the free protein ranged from 1.66 to 6.76 Å, whereas the geraniol-bound form exhibited improved stability, ranging from 1.65 to 5.07 Å. Furthermore, RMSF analysis across amino acid residues (Fig. 14B) indicated that geraniol binding induced local conformational fluctuations within acceptable limits, without compromising the overall structural integrity of either protein system.

Discussion

This study provides the first evidence that combined administration of geraniol and CoQ10 is associated with enhanced cardioprotection against myocardial I/R injury. While each compound conferred notable cardioprotection, their combination was accompanied by greater improvement in myocardial histoarchitecture and reduction of ST-segment elevation, infarct size, and injury biomarkers (CK-MB, cTn-1, LDH). To different extents, all treatments also counteracted apoptosis in association with modulation of the GSK-3β/β-catenin/Bcl-2/caspase-3 axis, restoring redox equilibrium, suppressing inflammatory cascades, and inhibiting ICAM-1/MPO hub, thereby reducing neutrophil infiltration and highlighting their potent anti-inflammatory effects.

Although animal I/R models do not fully emulate human STEMI complexity, they recapitulate key pathological features, including ischemia resulting from coronary artery obstruction, followed by blood flow restoration, which bizarrely aggravates myocardial impairment [4, 31]. Both also provoke ST-segment elevation, infarct formation, and elevated cardiac biomarkers, supporting their translational relevance to align with our findings and others [45, 46].

Reduction of infarct size represents a pivotal determinant in assessing cardioprotective efficacy during I/R injury [47]; accordingly, the ability of CoQ10 to minimize infarct size, associated with improved myocardial performance, underscores its cardioprotective effects to align with a prior report [48, 49]. Notably, although geraniol has not been previously explored in the context of I/R injury, our findings revealed its ability to diminish infarct size expansion to coincide with a previous evidence from isoproterenol-induced cardiotoxicity model, indicating its capacity to limit infarct extension and attenuate cardiac biomarker release [27], suggesting a potential cardioprotective profile.

On the molecular level, the GSK-3β/β-catenin cascade has been recognized as an important contributor to the pathophysiology of myocardial I/R injury [5, 14]. GSK-3β, a key regulatory kinase, governs β-catenin degradation and thereby influences multiple cellular processes relevant to cardiovascular integrity [50]. In

(See figure on next page.)

Fig. 5 Photomicrographs of myocardial tissue sections from rats subjected to I/R (H & E stain, X40 [left], and X80 [right]; n = 5 non-overlapped sections of 2 animals). Panels **A** & **B** display the normal histoarchitecture of the myocardial bundles [My] in the sham group, characterized by tightly aligned fibers with a transverse orientation, centrally located nuclei, intact blood vessels, and the absence of infiltrated inflammatory cells in the interstitial space. Conversely, the deleterious effects of I/R injury are evident in panels **C** & **D**, showing severe congestion in the myocardial blood vessels [V] along with focal infiltration of inflammatory cells [M] in the degenerated myocardium [D]. Pre-administration of either **E** & **F** geraniol or **G** & **H** CoQ10 markedly attenuated I/R-induced damage, as illustrated by the preservation of myocardial bundles, absence of vascular congestion, and reduced inflammatory infiltration. In line with biochemical findings, the section of **I** & **J** combined pre-administration of both agents provided the highest degree of myocardial protection against I/R insult

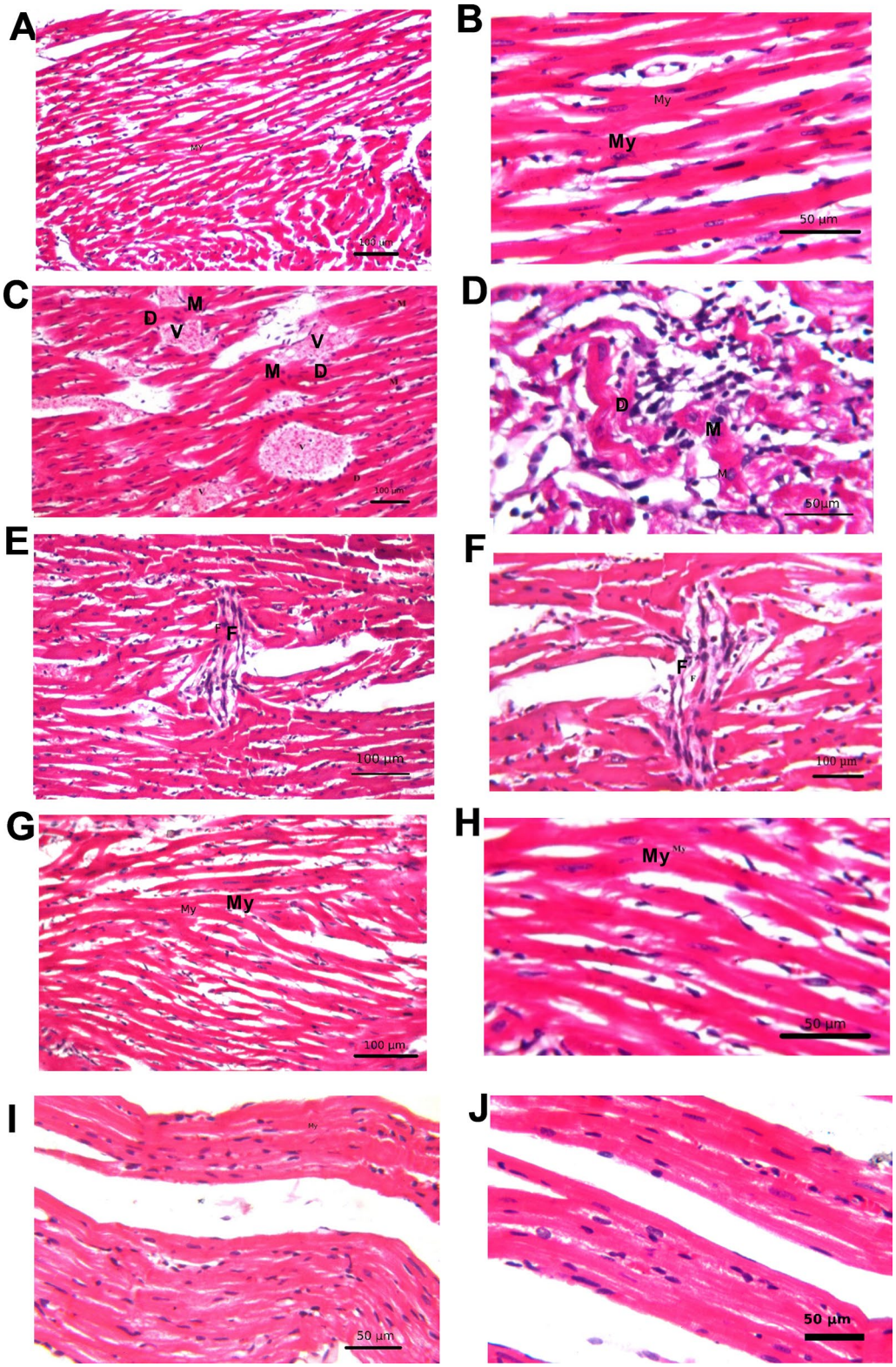

Fig. 5 (See legend on previous page.)

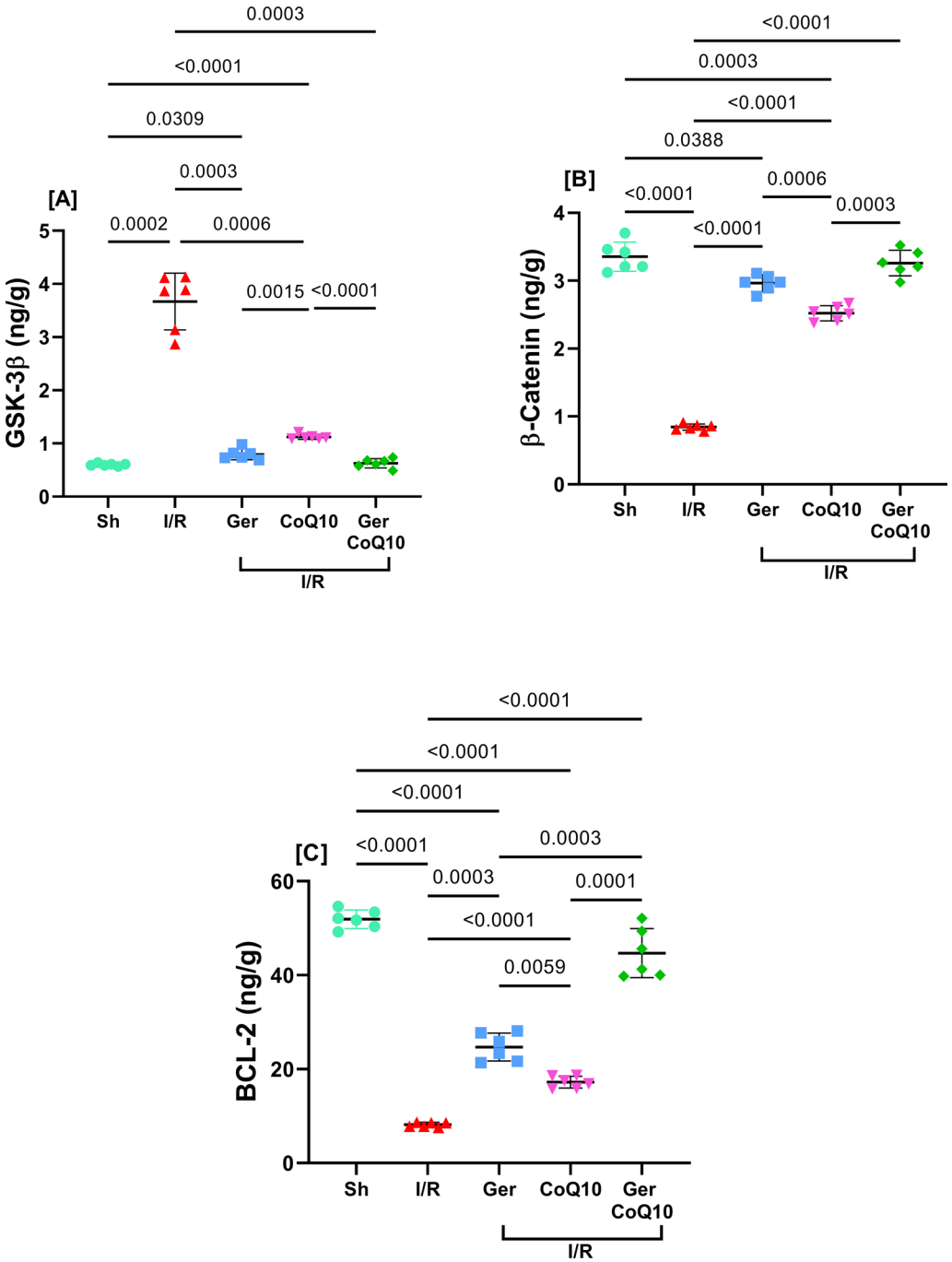

Fig. 6 Effect of preconditioning with geraniol and/or CoQ10 on myocardial contents of **A** GSK-3β, **B** β-catenin, and **C** Bcl-2 in rats subjected to I/R insult. Data of 6 observations were presented as mean ± SD. Welch's ANOVA test followed by Games-Howell's multiple comparison test was adopted to assess significant differences. A probability value (P) of less than 0.05 was considered statistically significant. Bcl-2: B-cell lymphoma-2; CoQ10: coenzyme Q10; GSK-3β: glycogen synthase kinase-3beta

the present study, the observed biochemical profile suggests a potential association between the cardioprotective effects of CoQ10 and/or geraniol and alterations in this axis. Specifically, the aptitude of these agents to reduce GSK-3β levels in parallel with increased β-catenin expression may indicate a possible involvement of this pathway in their cardioprotective potential, although direct evidence of pathway participation

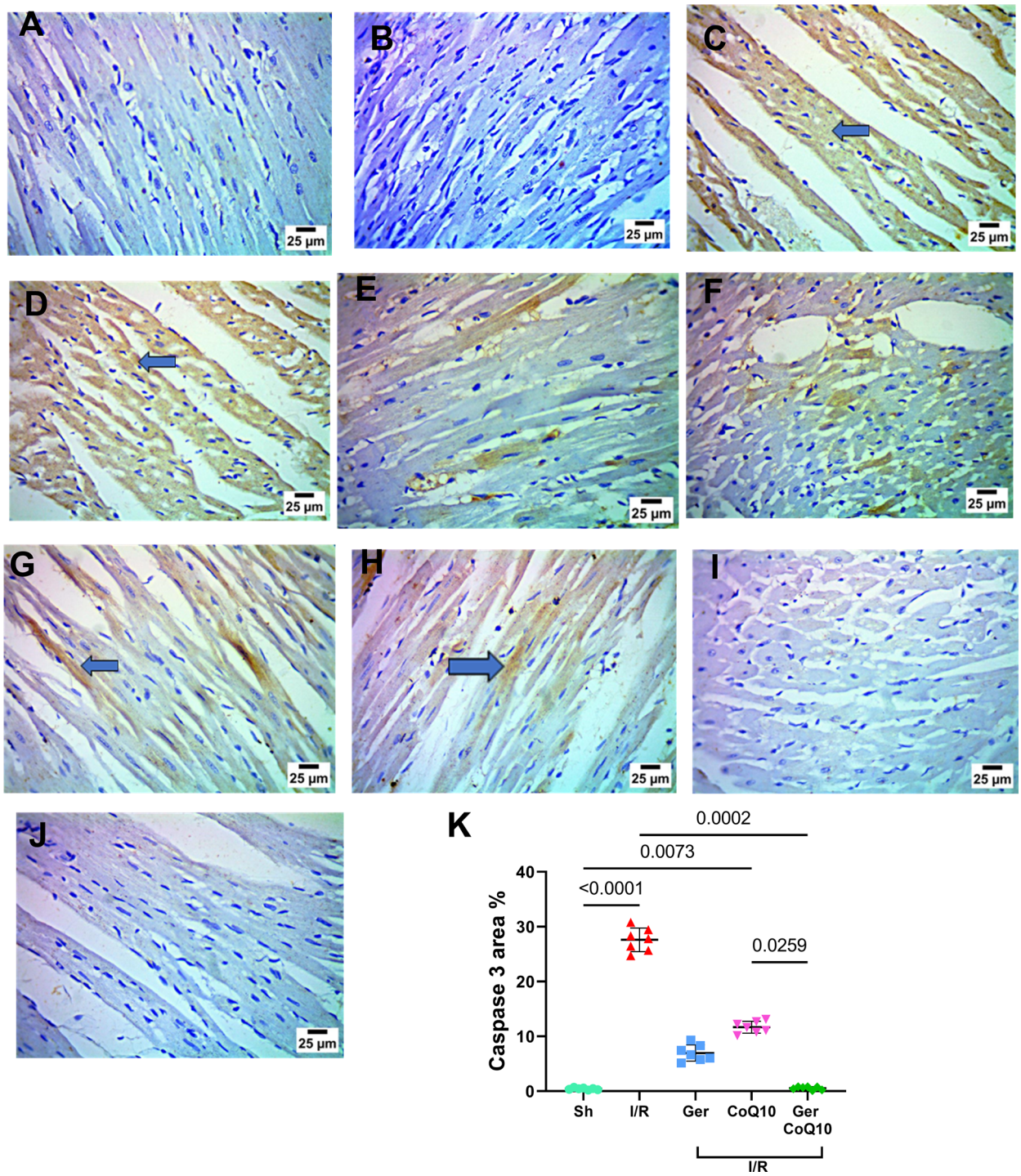

Fig. 7 Photomicrographs of caspase-3 immunostaining. **A**, **B** Sham panels showing negative expression of caspase 3 in cardiac muscle fibers, whereas **C**, **D** the I/R group revealing severe positive expression for the enzyme (arrow). Pretreatment with **E**, **F** geraniol shows mild positive expression of caspase 3 (arrow), while **G**, **H** the CoQ10 group shows moderate positive expression of caspase 3 (arrow). A negative immune expression of caspase-3 was detected in **I**, **J** the combination treated group. Panel **K** illustrates values of reaction area % of caspase 3 presented as means ± SD. Data were analyzed using one-way ANOVA followed by Tukey's post hoc test; $P < 0.05$. ANOVA, analysis of variance; CoQ10: coenzyme Q10; ger: geraniol; I/R: ischemia reperfusion; Sh: sham

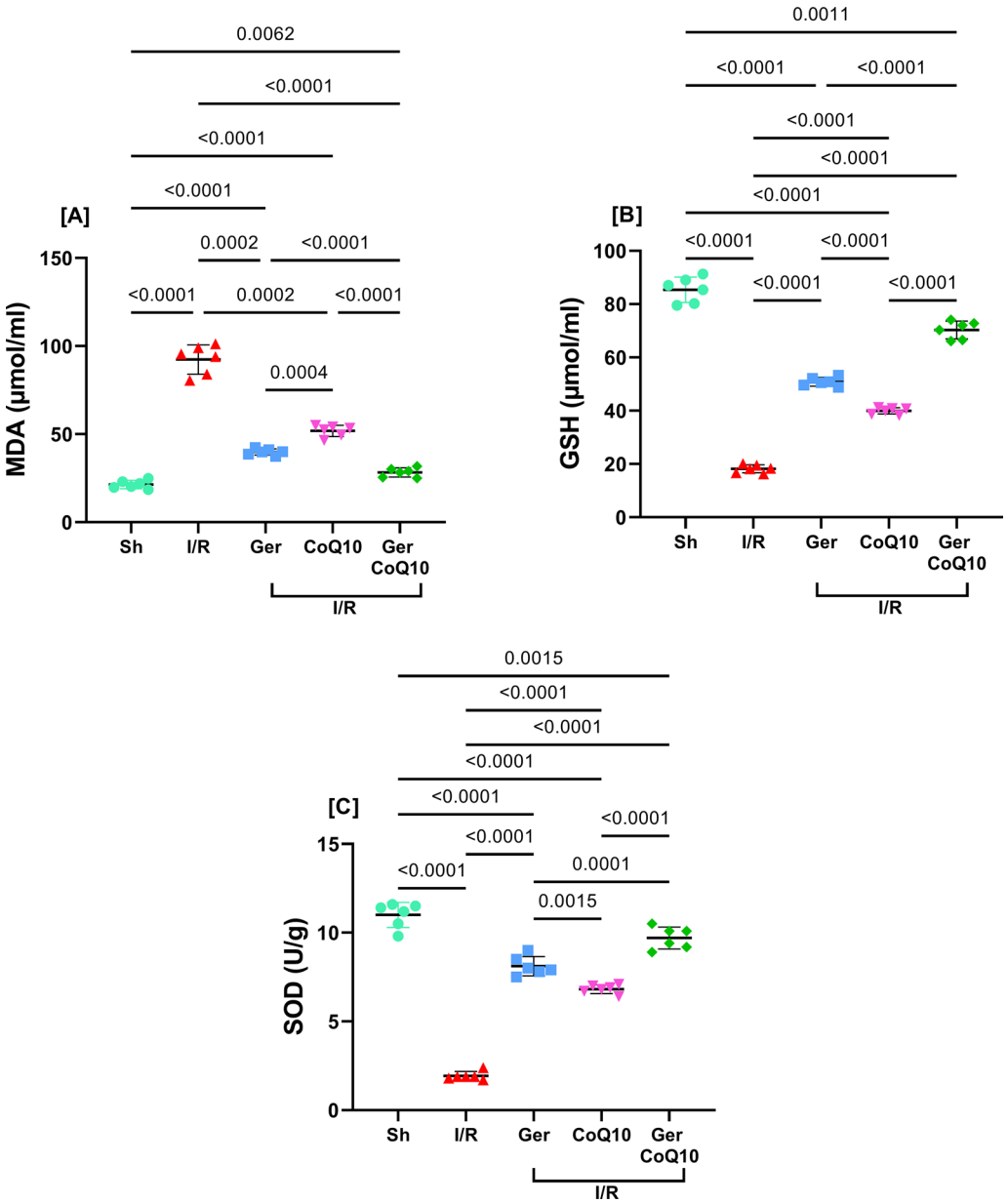

Fig. 8 Effect of pre-administration of geraniol and/or CoQ10 on myocardial contents of **A** MDA, **B** GSH, and **C** SOD activity in rats subjected to I/R injury. Data of 6 observations were presented as mean ± SD. One-way ANOVA followed by Tukey's post hoc test was adopted to assess significant differences. CoQ10: coenzyme Q10; MDA: malondialdehyde; GSH: reduced glutathione; SOD: superoxide dismutase

needs to be verified. In the same vein, former reports have shown that modulation of this pathway is linked to cardioprotective outcomes of naringenin [51] and aloperine [52], which preserved β-catenin levels while reducing GSK-3β activity. Moreover, activation of Wnt/β-catenin signaling has been reported to mitigate cardiac malformations induced by 4-tert-octylphenol [53]. In the same context, a recent review underscored GSK-3β inhibitors as particularly captivating therapeutic candidates due to their capacity to fine-tune pivotal molecular pathways implicated in myocardial I/R injury [5].

Moreover, the association between reduced GSK-3β activity and enhanced cardiac function, cardiomyocyte survival, and a decline in cardiac injury markers (cTn-I, LDH, CK-MB) has been recorded earlier [54, 55] to align with the present finding, where GSK-3β levels were observed to vary in parallel with these injury markers.

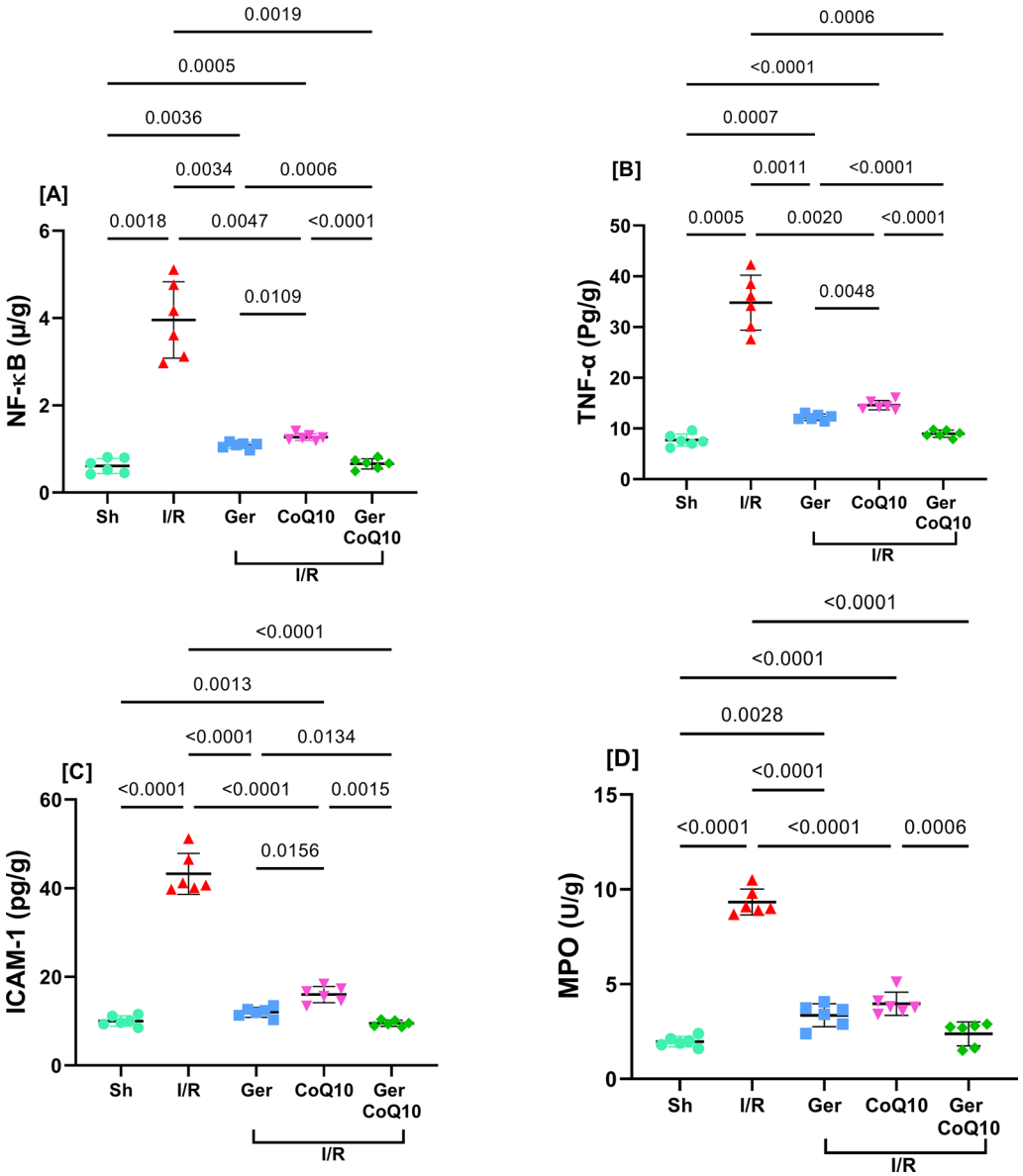

Fig. 9 Effect of pre-administration of geraniol and/or CoQ10 on myocardial contents of **A** p(S536) NF-κB, **B** TNF-α, **C** ICAM-1, and **D** MPO in rats subjected to I/R injury. Data of 6 observations were presented as mean ± SD. Welch's ANOVA test followed by Games-Howell's multiple comparison test was adopted to assess significant differences. A probability value (P) of less than 0.05 was considered statistically significant. CoQ10: coenzyme Q10; ICAM-1: intercellular adhesion molecule-1; MPO: myeloperoxidase; p(S536)-NF-κB: phosphorylated nuclear factor kappa B at serine 536; TNF-α: tumor necrosis factor alpha

Additionally, higher GSK-3β levels were associated with amplified oxidative stress, inflammation, and apoptosis, whereas treatment with the examined agents coincided with attenuation of these alterations, highlighting their antioxidant, anti-inflammatory, and antiapoptotic capacities. Moreover, elevated GSK-3β levels correlated positively with MDA, MPO, ICAM-1, TNF-α, and NF-κB, whereas negative correlations were observed with antioxidant defenses (GSH, SOD) and the antiapoptotic marker Bcl-2. Furthermore, GSK-3β exhibited an inverse relationship with β-catenin, which in turn negatively correlated with NF-κB, in agreement with a previous report in a hepatic I/R model [56]. Collectively, these findings support an association between the GSK-3β/β-catenin axis and myocardial injury-related processes; however, they do not establish a direct mechanistic role in the current experimental setting.

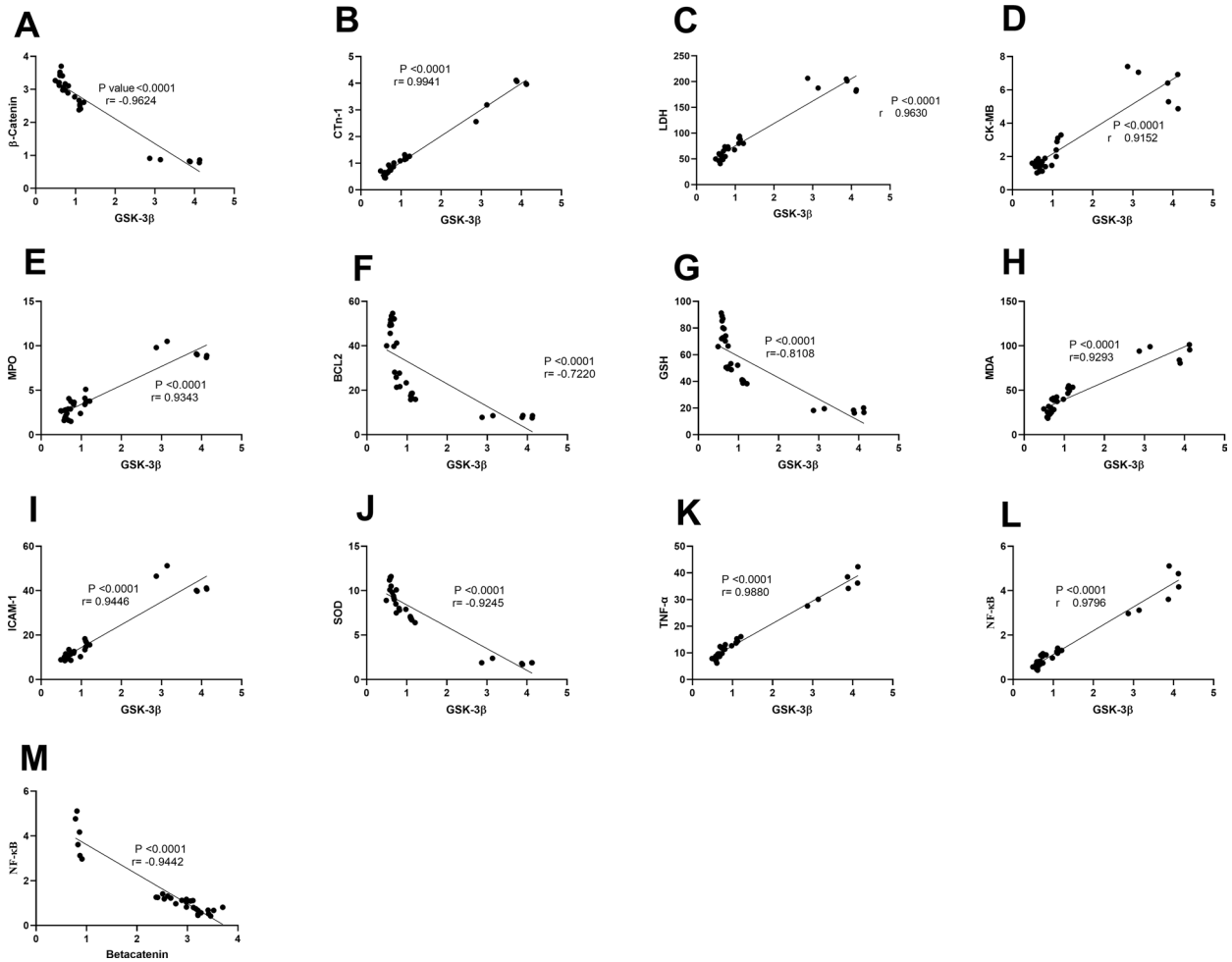

Fig. 10 Person's correlation coefficient analysis ($P < 0.0001$) shows strong positive correlations between strong negative correlations between GSK-3β and **A** β-catenin, **F** Bcl-2, **G** GSH, **J** SOD with strong positive correlations between GSK-3β and **B** cTn-1, **C** LDH, **D** CK-MB, **E** MPO, **H** MDA, **I** ICAM-1, **K** TNF-alpha, and **L** NF-κB. Meanwhile, β-catenin has strong negative associates with **M** NF-κB. Bcl-2: B-cell lymphoma 2; CK-MB: creatine kinase–MB isoenzyme; cTn-1: cardiac Troponin I; GSH: reduced glutathione; *p*-GSK3β: glycogen synthase kinase-3 beta phosphorylated at serine 9; ICAM-1: intercellular adhesion molecule 1; LDH: lactate dehydrogenase; MDA: malondialdehyde; MPO: myeloperoxidase; p(S536)-NF-κB: nuclear factor kappa B phosphorylated at serine 536; SOD: superoxide dismutase; TNF-α: tumor necrosis factor alpha; r, Pearson's correlation coefficient

During reperfusion, excessive ROS generation and inflammatory responses exacerbate myocardial damage. ROS promote lipid peroxidation [57], overwhelm antioxidant defenses [57, 58], and impair myocardial function [59]. In the present study, geraniol and CoQ10, particularly in combination, were associated with reduced lipid peroxidation and restoration of GSH and SOD, consistent with their antioxidative effects reported in non-cardiac [26, 60] and cardiac injury models [19, 27, 49, 61, 62]. Although these effects coincided with changes in GSK-3β and β-catenin, a direct mechanistic link needs to be established. Previous evidence suggests that GSK-3β may contribute to mitochondrial dysfunction and ROS generation [63] and redox imbalance [64], while β-catenin elevation mitigates ROS [65].

Beyond oxidative damage, ROS trigger inflammatory cascades via cytokine induction [9]. In line with this, I/R elevated NF-κB and TNF-α, while treatment with geraniol and/or CoQ10 coincided with reductions in these markers, supporting their anti-inflammatory profile, as previously reported [27, 66]. Notably, GSK-3β has been previously implicated in the modulation of inflammatory pathways, including those involving NF-κB and downstream cytokine expression [14, 67, 68]. Moreover, GSK-3β has been linked to inflammatory regulation in other models, including hepatocyte injury and TNF-α-mediated responses [69]. In line with

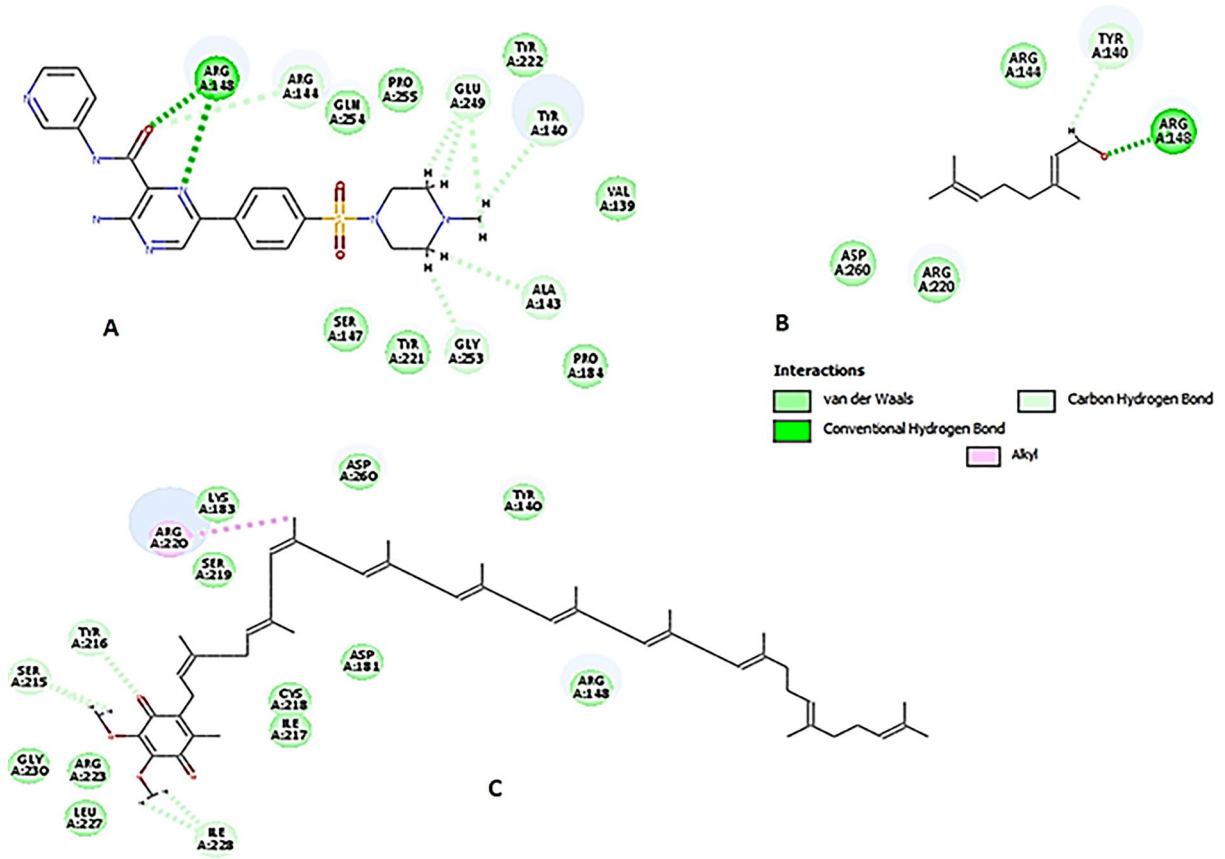

Fig. 11 2D interaction against GSK-3β: **A** Reference GR9, **B** geraniol, and (**C**) CoQ10, provided with color map for interactions. CoQ10: coenzyme Q10; GSK-3β: glycogen synthase kinase-3 beta

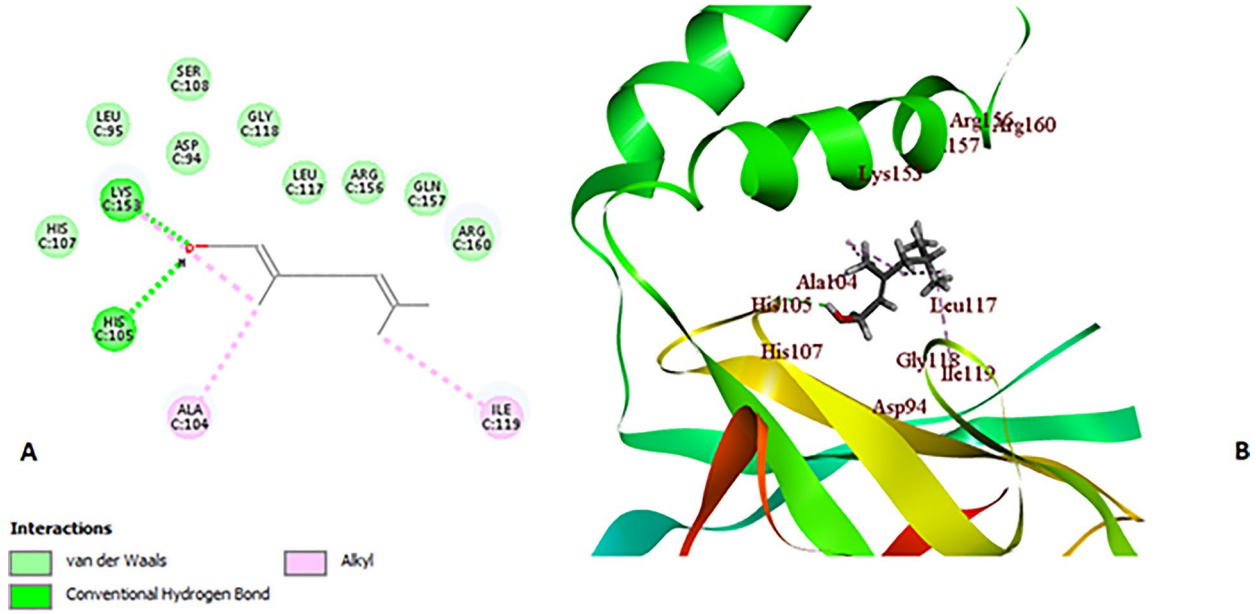

Fig. 12 Interaction of geraniol against NF-κB. **A** 2D interaction diagram, **B** 3D interaction diagram. NF-κB: nuclear factor kappa B

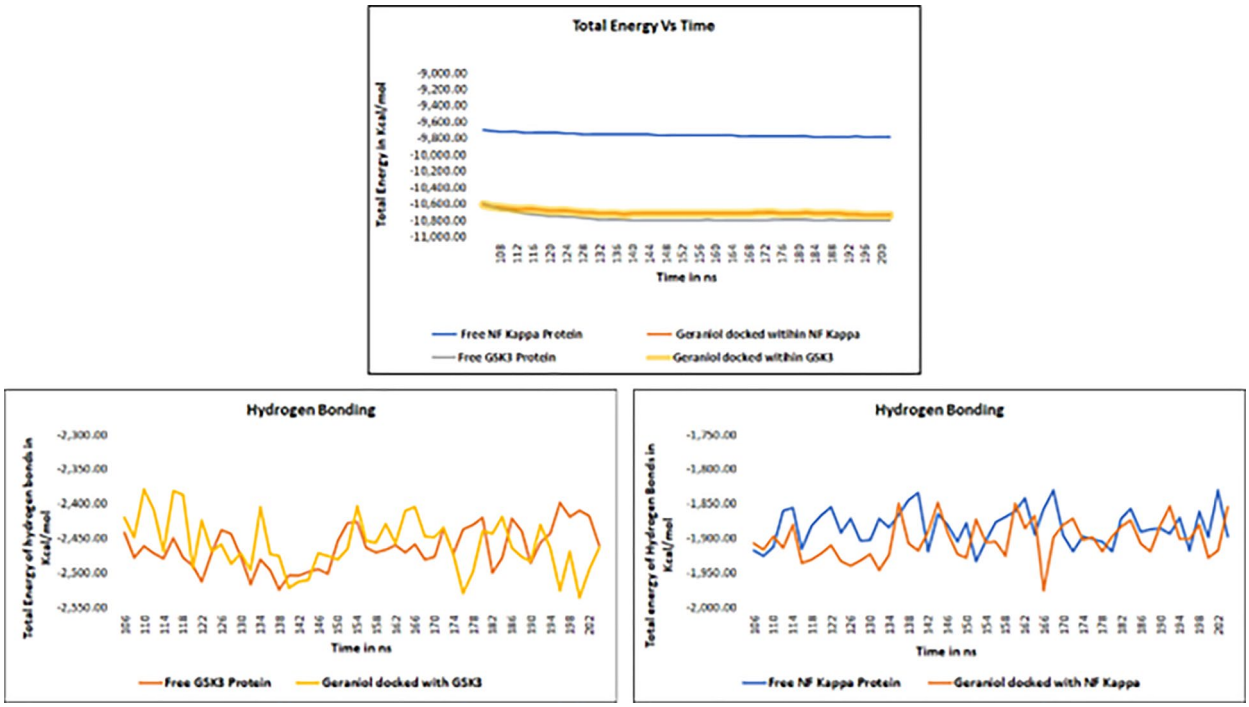

Fig. 13 Comparative graphical data for dynamic simulation studies results. Analysis of hydrogen bonding further supported the enhanced stability of the geraniol–protein complexes. Free GSK-3β exhibited hydrogen bonding energies between – 2397 and – 2524 kcal/mol, which slightly increased upon geraniol binding (– 2378 to – 2535 kcal/mol), indicating additional stabilizing interactions. Likewise, the hydrogen bonding energy of free NF-κB (– 1829 to – 1933 kcal/mol) increased in the presence of geraniol (– 1848 to – 1975 kcal/mol)

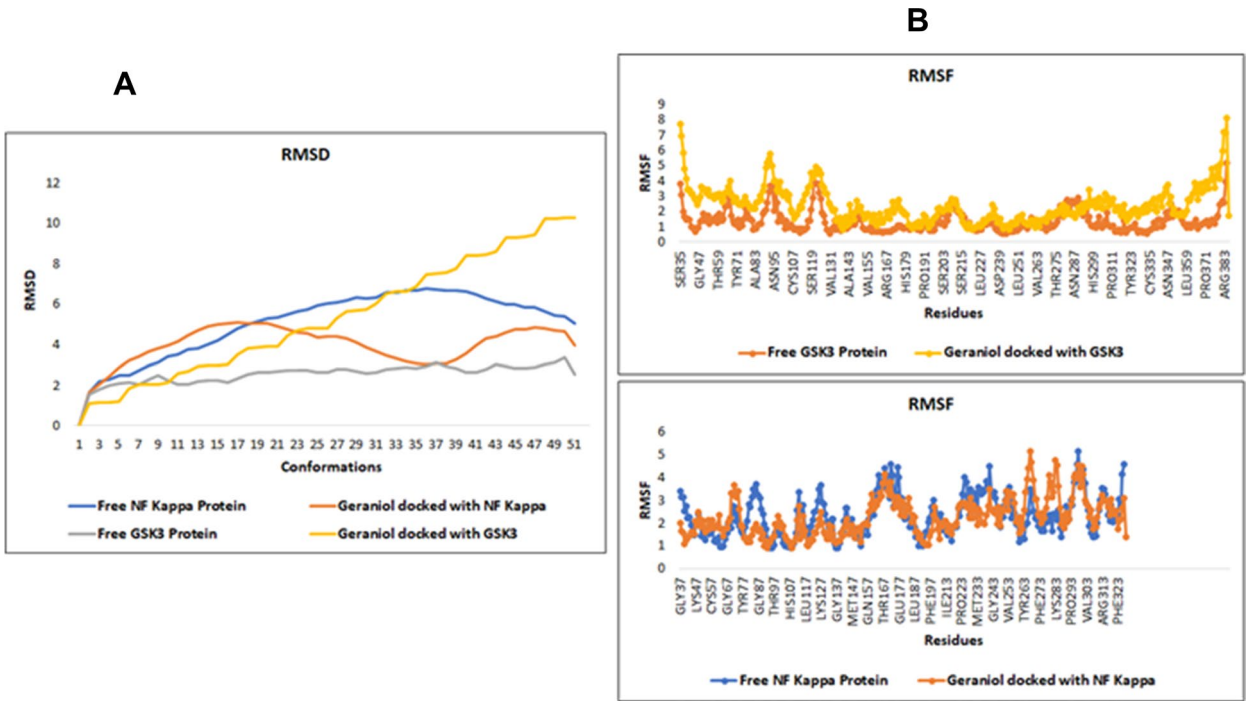

Fig. 14 Comparable graphical data for results of trajectory analysis. **A** RMSD and **B** RMSF. RMSD: root-mean-square deviation; RMSF: root-mean-square fluctuation

this, the present data demonstrated that NF-κB levels were elevated in the I/R model and positively correlated with GSK-3β, while treatment with geraniol and/or CoQ10 coincided with reductions in both markers, further supporting a potential association between GSK-3β-related signaling and inflammatory responses under these conditions.

Oxidative stress and inflammation also contribute to endothelial dysfunction and neutrophil infiltration [70]. Consistently, I/R increased ICAM-1 expression and MPO activity [71], reflecting enhanced neutrophil recruitment [72]. The ability of geraniol and CoQ10 to attenuate these markers was associated with reduced inflammatory burden to coincide with previous studies showing reduced ICAM-1 and MPO in various models [23, 26, 73, 74]. Given the established contribution of neutrophils to infarct expansion [75, 76], these findings may partly explain the observed reduction in infarct size and improved cardiac function [77], although causality cannot be inferred. The role of GSK-3β in modulating neutrophils' infiltration cannot be ruled out, where an earlier study proved that inhibition of this kinase resulted in a decrease in both ICAM-1 and MPO [78]. Whether this holds true for geraniol and/or CoQ10 needs to be proven.

Myocardial I/R induces cardiomyocyte demise is mediated through apoptosis and/or necrosis, with apoptosis being the predominant mode [79], regulated by Bcl-2 family proteins [80]. In the present study, preconditioning with any of the tested agents and especially their combination opposed the apoptotic role of I/R and increased Bcl-2 while reduced caspase-3, indicating their antiapoptotic potentials, consistent with prior reports for geraniol [26] and CoQ10 [81]. The protective role of Bcl-2 in limiting ischemic injury has been previously demonstrated [82], which may be partly related to the modulation of GSK-3β/β-catenin axis. This notion was verified earlier, where previous studies suggest that GSK-3β activity is linked to apoptotic signaling [82], and that increased β-catenin may influence Bcl-2 expression [12].

Furthermore, the inhibitory interaction of geraniol on GSK-3β was examined in silico and comparatively evaluated against CoQ10 to clarify its mechanism of action. Consistent with the biochemical pattern demonstrating the superior efficacy of geraniol over CoQ10, molecular docking and dynamics analyses revealed that geraniol effectively occupied the inhibitory binding site of GSK-3β through key hydrogen bonds with Tyr140 and Arg148, whereas CoQ10 interacted with less relevant residues distant from the active site. Moreover, molecular dynamics simulations and trajectory analyses revealed that the geraniol-GSK-3β complex exhibited stability comparable to that of the free protein. The formation of hydrogen bonds and the observed stable fluctuations suggest that geraniol might induce conformational changes in GSK-3β that may be associated with effective inhibition. Likewise, geraniol, but not CoQ10, successfully bound the inhibitory site of NF-κB, further confirming the concordance between the computational and experimental findings and the molecular dynamics simulations and trajectory analyses further confirmed the high stability of the geraniol-NF-κB complex relative to the free NF-κB protein. The RMSD values remained low and consistent, and the fluctuations were steady throughout the simulation period. These findings indicate the formation of stable hydrogen bonds between geraniol and NF-κB, suggesting potential structural and functional changes consistent with inhibitory activity.

Although the study offers important observations, some limitations merit consideration. The use of a pretreatment experimental design may limit direct clinical translation to acute myocardial infarction settings, where interventions are typically administered after ischemic onset. In addition, allocation of animals to different endpoints resulted in relatively small sample sizes for certain assays (e.g., histology and area at risk), which may influence the robustness of these outcomes despite alignment with common practice in I/R studies. Although alterations in GSK-3β and β-catenin were observed, the absence of direct mechanistic validation precludes definitive conclusions regarding the underlying mechanisms, and thus the findings should be interpreted as associative rather than causal. Furthermore, the use of a single animal species and sex may limit generalizability across biological contexts. The lack of long-term outcome assessment also precludes conclusions regarding sustained cardioprotective effects or potential delayed adverse consequences.

Conclusion

Our investigation is the first to highlight the cardioprotective potential of geraniol, either independently or in synergy with CoQ10, in mitigating myocardial I/R-induced damage, with their combination exhibiting superior efficacy. Additionally, this study accentuates a potential association between modulation of GSK-3β and attenuation of I/R-driven pathological events, including inflammatory responses, oxidative stress, neutrophil infiltration, and apoptotic cell loss. These coordinated changes were accompanied by reduced infarct size, diminished ST-segment elevation, lower cardiac biomarkers, and preservation of myocardial histoarchitecture, supporting the therapeutic potential of this combinatorial approach. However, further studies are required to validate the direct involvement of GSK-3β in these cascades and to elucidate the mechanistic basis

underlying the cardioprotective effects of geraniol and CoQ10. Future investigations should focus on defining the precise molecular mechanisms of their potential synergy, evaluating long-term outcomes, and assessing their translational relevance in clinically representative models.

Abbreviations

AAR	Area at risk
ACS	Acute coronary syndrome
AMI	Acute myocardial infarction
ANOVA	Analysis of variance
β-catenin	Beta-catenin
Bcl-2	B-cell lymphoma 2
CK-MB	Creatine kinase-MB
CoQ10	Coenzyme Q10
cTn-I	Cardiac troponin I
ECG	Electrocardiography
ELISA	Enzyme-linked immunosorbent assay
GSH	Reduced glutathione
GSK-3β	Glycogen synthase kinase-3β
H&E	Hematoxylin and eosin
HMG-CoA	3-Hydroxy-3-methylglutaryl coenzyme A
I/R	Ischemia/reperfusion
ICAM-1	Intercellular adhesion molecule-1
IHC	Immunohistochemistry
LAD	Left anterior descending (coronary artery)
LDH	Lactate dehydrogenase
MDA	Malondialdehyde
MPO	Myeloperoxidase
NF-κB	Nuclear factor kappa B
NVT	Number of particles, volume, and temperature
RMSD	Root-mean-square deviation
RMSF	Root-mean-square fluctuation
ROS	Reactive oxygen species
SD	Standard deviation
SOD	Superoxide dismutase
STEMI	ST-elevation myocardial infarction
TNF-α	Tumor necrosis factor alpha
TTC	2,3,5-Triphenyltetrazolium chloride

Author contributions

N. F. E. helped in writing—original draft, software, resources, methodology, formal analysis, data curation, conceptualization, software, funding, investigation. A. S. A. contributed to supervision, resources, data curation, software, conceptualization. I. M. F. was involved in conceptualization, methodology, data curation, formal analysis, software, visualization, investigation, writing—original draft. H. M. M. helped in writing—original draft, methodology, resources. H. S. E. contributed to writing—original draft, writing—review & editing, visualization, software, resources, formal analysis, data curation, conceptualization, supervision.

Funding

This research did not receive any specific grant from funding agencies in the public, commercial, or not-for-profit sectors.

Availability of data and materials

The data that support the findings of this study are available on a reasonable request from the corresponding author.

Declarations

Ethics approval and consent to participate

This study adheres to the ARRIVE guidelines and the *Guide for the Care and Use of Laboratory Animals* issued by the US National Institutes of Health (NIH Publication No. 85-23, revised 1996) and has received ethical clearance from the Research Ethics Committee of the Faculty of Pharmacy, Cairo University, Cairo, Egypt (Permit Number: PT 1110).

Consent for publication

Not applicable.

Competing interest

The corresponding author on behalf of the other co-authors declares having no conflict of interest that can influence the submitted work.

Author details

[1]Department of Pharmacology & Toxicology, Faculty of Pharmacy, Ahram Canadian University, Giza, Egypt. [2]Department of Pharmacology & Toxicology, Faculty of Pharmacy, Al-Azhar University, Cairo, Egypt. [3]Department of Pharmaceutical Chemistry, Faculty of Pharmacy, Future University in Egypt, Cairo 11835, Egypt. [4]Medical Pharmacology Department, Faculty of Medicine, Cairo University, Cairo, Egypt. [5]Department of Pharmacology, Toxicology, and Biochemistry, Faculty of Pharmacy, Future University in Egypt, Cairo, Egypt.

Received: 4 February 2026 Accepted: 24 April 2026
Published online: 13 May 2026

References

1. Abdul Jabbar AB, Klisares M, Gilkeson K, Aboeata A (2025) Acute myocardial infarction mortality in the older population of the United States: an analysis of demographic and regional trends and disparities from 1999 to 2022. J Clin Med 14(7):2190. https://doi.org/10.3390/jcm14072190
2. Kryeziu B, Poniku A, Henein MY et al (2026) Epidemiological 11-year dynamics study of acute myocardial infarction: a cohort study in a country with a transitional healthcare system. Glob Heart 21(1):14. https://doi.org/10.5334/gh.1525
3. Riascos-Bernal DF, Quinones G, Abdelaal SA et al (2026) Pathogenesis of plaque erosion. Trends Cardiovasc Med 36(2):105–112. https://doi.org/10.1016/j.tcm.2025.09.004
4. Mechanic OJ, Gavin M, Grossman SA (2026) Acute myocardial infarction. In: StatPearls. StatPearls Publishing, Treasure Island (FL)
5. Ghanta SN, Kattamuri LPV, Odueke A, Mehta JL (2025) Molecular insights into ischemia-reperfusion injury in coronary artery disease: mechanisms and therapeutic implications: a comprehensive review. Antioxidants 14(2):213. https://doi.org/10.3390/antiox14020213
6. Pastena P, Frye JT, Ho C et al (2024) Ischemic cardiomyopathy: epidemiology, pathophysiology, outcomes, and therapeutic options. Heart Fail Rev 29(1):287–299. https://doi.org/10.1007/s10741-023-10377-4
7. Li F-J, Hsu T, Li H-X et al (2014) Protective effect and mechanism of lithium chloride pretreatment on myocardial ischemia-reperfusion injury in rats. Asian Pac J Trop Med 7(9):744–748. https://doi.org/10.1016/S1995-7645(14)60128-0
8. Maxwell SR (1997) Anti-oxidant therapy: does it have a role in the treatment of human disease? Expert Opin Investig Drugs 6(3):211–236. https://doi.org/10.1517/13543784.6.3.211
9. Frangogiannis NG, Smith CW, Entman ML (2002) The inflammatory response in myocardial infarction. Cardiovasc Res 53(1):31–47. https://doi.org/10.1016/S0008-6363(01)00434-5
10. Hermans KC, Daskalopoulos EP, Blankesteijn WM (2012) Interventions in Wnt signaling as a novel therapeutic approach to improve myocardial infarct healing. Fibrogenesis Tissue Repair 5(1):16. https://doi.org/10.1186/1755-1536-5-16
11. Rayasam GV, Tulasi VK, Sodhi R et al (2009) Glycogen synthase kinase 3: more than a namesake. Br J Pharmacol 156(6):885–898. https://doi.org/10.1111/j.1476-5381.2008.00085.x
12. Kaga S, Zhan L, Altaf E, Maulik N (2006) Glycogen synthase kinase-3β/β-catenin promotes angiogenic and anti-apoptotic signaling through the induction of VEGF, Bcl-2 and survivin expression in rat ischemic preconditioned myocardium. J Mol Cell Cardiol 40(1):138–147. https://doi.org/10.1016/j.yjmcc.2005.09.009
13. Thirunavukkarasu M, Han Z, Zhan L et al (2008) Adeno-sh-beta-catenin abolishes ischemic preconditioning-mediated cardioprotection by downregulation of its target genes VEGF, Bcl-2, and survivin in ischemic rat myocardium. Antioxid Redox Signal 10(8):1475–1484. https://doi.org/10.1089/ars.2008.2042
14. Meco M, Giustiniano E, Nisi F et al (2025) MAPK, PI3K/Akt pathways, and GSK-3β activity in severe acute heart failure in intensive care patients: an

updated review. J Cardiovasc Dev Dis 12(7):266. https://doi.org/10.3390/jcdd12070266
15. Demarchi F, Bertoli C, Sandy P, Schneider C (2003) Glycogen synthase kinase-3 beta regulates NF-kappa B1/p105 stability. J Biol Chem 278(41):39583–39590. https://doi.org/10.1074/jbc.M305676200
16. Zhai P, Sciarretta S, Galeotti J et al (2011) Differential roles of GSK-3β during myocardial ischemia and ischemia/reperfusion. Circ Res 109(5):502–511. https://doi.org/10.1161/CIRCRESAHA.111.249532
17. Almalki SG, Alsaweed M, Muteb Albadrani H et al (2024) A molecular informatics and in-vitro approach to evaluate the HMG-CoA reductase inhibitory efficacy of monoterpenes, carvacrol and geraniol. J Taibah Univ Sci 18(1):2297456. https://doi.org/10.1080/16583655.2023.2297456
18. Ben Ammar R (2023) Potential effects of Geraniol on cancer and inflammation-related diseases: a review of the recent research findings. Molecules 28(9):3669. https://doi.org/10.3390/molecules28093669
19. Ben Ammar R, Abdulaziz Alamer S, Elsayed Mohamed M et al (2024) Potential inhibitory effect of geraniol isolated from lemongrass (*Cymbopogon commutatus* Stapf) on tilmicosin-induced oxidative stress in cardiac tissue. Nat Prod Res 38(10):1652–1661. https://doi.org/10.1080/14786419.2023.2215901
20. Ghirlanda G, Oradei A, Manto A et al (1993) Evidence of plasma CoQ10-lowering effect by HMG-CoA reductase inhibitors: a double-blind, placebo-controlled study. J Clin Pharmacol 33(2):226–229
21. Seneş M, Erbay AR, Yilmaz FM et al (2008) Coenzyme Q10 and high-sensitivity C-reactive protein in ischemic and idiopathic dilated cardiomyopathy. Clin Chem Lab Med 46(3):382–386. https://doi.org/10.1515/CCLM.2008.061
22. Pallotti F, Bergamini C, Lamperti C, Fato R (2021) The roles of Coenzyme Q in disease: direct and indirect involvement in cellular functions. Int J Mol Sci 23(1):128. https://doi.org/10.3390/ijms23010128
23. Mirmalek SA, Gholamrezaei Boushehrinejad A, Yavari H et al (2016) Antioxidant and anti-inflammatory effects of Coenzyme Q10 on L-Arginine-induced acute pancreatitis in rat. Oxid Med Cell Longev. https://doi.org/10.1155/2016/5818479
24. Jin H, Fedorowicz G, Yang R et al (2004) Thyrotropin-releasing hormone is induced in the left ventricle of rats with heart failure and can provide inotropic support to the failing heart. Circulation 109(18):2240–2245. https://doi.org/10.1161/01.CIR.0000127951.13380.B4
25. Zhao M, Yang J, Wang X et al (2013) The PI3K/Akt pathway mediates the protection of SO2 preconditioning against myocardial ischemia/reperfusion injury in rats. Acta Pharmacol Sin 34(4):501–506. https://doi.org/10.1038/aps.2012.204
26. Khoshnazar SM, Mohagheghi M, Rahimi S et al (2025) Geraniol modulates inflammatory and antioxidant pathways to mitigate intestinal ischemia-reperfusion injury in male rats. Naunyn Schmiedebergs Arch Pharmacol 398(7):8713–8727. https://doi.org/10.1007/s00210-025-03802-y
27. Zou G, Wan J, Balupillai A et al (2022) Geraniol enhances peroxiredoxin-1, and prevents isoproterenol-induced oxidative stress and inflammation associated with myocardial infarction in experimental animal models. J Biochem Mol Toxicol 36(8):e23098. https://doi.org/10.1002/jbt.23098
28. Akinmoladun AC, Saliu I, Abilogun O et al (2022) Comparative influence of kolaviron and coenzyme Q10 on complex I activity, glutamate clearance, 3,4-dihydroxyphenethylamine metabolism, and redox stress in rotenone-induced neurotoxicity. Niger J Physiol Sci 37(2):165–173. https://doi.org/10.54548/njps.v37i2.2
29. Lamia SS, Emran T, Rikta JK et al (2021) Coenzyme Q10 and Silymarin reduce CCl4-induced oxidative stress and liver and kidney injury in ovariectomized rats—implications for protective therapy in chronic liver and kidney diseases. Pathophysiology 28(1):50–63. https://doi.org/10.3390/pathophysiology28010005
30. Wang H, Cao C, Hui L et al (2016) A study of myocardial ischemia model induced by left coronary artery ligation in rats. World J Cardiovasc Dis 6(5):133–142. https://doi.org/10.4236/wjcd.2016.65014
31. Xiao H, Liu J, Cai Q et al (2025) Maresin 1 alleviates myocardial ischemia-reperfusion injury in rats by suppressing inflammation. Eur J Histochem 69(4):4254. https://doi.org/10.4081/ejh.2025.4254
32. Preda MB, Burlacu A (2010) Electrocardiography as a tool for validating myocardial ischemia–reperfusion procedures in mice. Comp Med 60(6):443–447
33. Hasegawa S, Kusuoka H, Fukuchi K et al (2000) Estimation of the area at risk in myocardial infarction of rats by means of I-123 β-methyliodophenyl pentadecanoic acid imaging. Ann Nucl Med 14(5):347–352. https://doi.org/10.1007/BF02988694
34. Wang Y, Liu L, Hu C, Cheng Y (2007) Effects of Salviae Mitiorrhizae and Cortex Moutan extract on the rat heart after myocardial infarction: a proteomic study. Biochem Pharmacol 74(3):415–424. https://doi.org/10.1016/j.bcp.2007.04.017
35. Fishbein MC, Meerbaum S, Rit J et al (1981) Early phase acute myocardial infarct size quantification: validation of the triphenyl tetrazolium chloride tissue enzyme staining technique. Am Heart J 101(5):593–600
36. Briet F, Keith M, Leong-Poi H et al (2008) Triple nutrient supplementation improves survival, infarct size and cardiac function following myocardial infarction in rats. Nutr Metab Cardiovasc Dis 18(10):691–699. https://doi.org/10.1016/j.numecd.2007.10.003
37. Sahna E, Acet A, Kaya Ozer M, Olmez E (2002) Myocardial ischemia–reperfusion in rats: reduction of infarct size by either supplemental physiological or pharmacological doses of melatonin. J Pineal Res 33(4):234–238. https://doi.org/10.1034/j.1600-079X.2002.02924.x
38. Köksal Z, Kurtipek Ö, Arslan M et al (2023) Protective effects of hydrogen rich saline solution in rats with experimental myocardial ischemia reperfusion injury. Heliyon 9(12):e22973. https://doi.org/10.1016/j.heliyon.2023.e22973
39. Krawisz JE, Sharon P, Stenson WF (1984) Quantitative assay for acute intestinal inflammation based on myeloperoxidase activity. Assessment of inflammation in rat and hamster models. Gastroenterology 87(6):1344–1350
40. Gupta P, Kanwal A, Putcha UK et al (2013) Cardioprotective effect of ritonavir, an antiviral drug, in isoproterenol induced myocardial necrosis: a new therapeutic implication. J Transl Med 11(1):80. https://doi.org/10.1186/1479-5876-11-80
41. Berg S, Bergh M, Hellberg S et al (2012) Discovery of novel potent and highly selective glycogen synthase kinase-3β (GSK3β) inhibitors for Alzheimer's disease: design, synthesis, and characterization of pyrazines. J Med Chem 55(21):9107–9119. https://doi.org/10.1021/jm201724m
42. Cramer P, Larson CJ, Verdine GL, Müller CW (1997) Structure of the human NF-κB p52 homodimer-DNA complex at 2.1 A resolution. EMBO J 16(23):7078–7090. https://doi.org/10.1093/emboj/16.23.7078
43. Ali GME, Ewida MA, Elmetwali AM et al (2024) Discovery of pyrazole-based analogs as CDK2 inhibitors with apoptotic-inducing activity: design, synthesis and molecular dynamics study. RSC Adv 14(47):34537–34555. https://doi.org/10.1039/d4ra06500j
44. Joelijanto R, Sutjiati R (2025) Antibacterial activity of ethanol extract of cocoa beans (*Theobroma cacao* L): In silico and in vitro study. J Dentomaxillofac Sci 10(4):198–202. https://doi.org/10.15562/jdmfs.v10i4.1884
45. Smith SC, Allen J, Blair SN et al (2006) AHA/ACC guidelines for secondary prevention for patients with coronary and other atherosclerotic vascular disease: 2006 update. Circulation 113(19):2363–2372. https://doi.org/10.1161/CIRCULATIONAHA.106.174516
46. Cheng Y-H, Chiang C-Y, Wu C-H, Chien C-T (2024) 2′-Hydroxycinnamaldehyde, a natural product from cinnamon, alleviates ischemia/reperfusion-induced microvascular dysfunction and oxidative damage in rats by upregulating cytosolic BAG3 and Nrf2/HO-1. Int J Mol Sci 25(23):12962. https://doi.org/10.3390/ijms252312962
47. Csonka C, Kupai K, Kocsis GF et al (2010) Measurement of myocardial infarct size in preclinical studies. J Pharmacol Toxicol Methods 61(2):163–170. https://doi.org/10.1016/j.vascn.2010.02.014
48. Awad K, Sayed A, Banach M (2022) Coenzyme Q10 reduces infarct size in animal models of myocardial ischemia-reperfusion injury: a meta-analysis and summary of underlying mechanisms. Front Cardiovasc Med 9:857364. https://doi.org/10.3389/fcvm.2022.857364
49. Bafadam S, Mokhtari B, Vafaee MS et al (2024) Mitochondrial transplantation combined with coenzyme Q10 induces cardioprotection and mitochondrial improvement in aged male rats with reperfusion injury. Exp Physiol 110(5):744–754. https://doi.org/10.1113/EP091358
50. Cheng H, Woodgett J, Maamari M, Force T (2011) Targeting GSK-3 family members in the heart: a very sharp double-edged sword. J Mol Cell Cardiol 51(4):607–613. https://doi.org/10.1016/j.yjmcc.2010.11.020
51. Guo X, Ji Q, Wu M, Ma W (2022) Naringin attenuates acute myocardial ischemia-reperfusion injury via miR- 126/GSK-3β/β-catenin signaling pathway. Acta Cir Bras 37(1):e370102. https://doi.org/10.1590/acb370102
52. Wei S, Ju F, Xiao J et al (2024) Aloperine alleviates myocardial injury induced by myocardial ischemia and reperfusion by activating the

ERK1/2/β-catenin signaling pathway. Cardiovasc Drugs Ther 39(3):533–551. https://doi.org/10.1007/s10557-024-07566-0
53. Wang X, Chen J, Hu H et al (2025) The resveratrol attenuates reactive oxygen species mediated DNA damage in cardiac malformations caused by 4-tert-octylphenol. Toxicol Appl Pharmacol 498:117284. https://doi.org/10.1016/j.taap.2025.117284
54. Padrón-Barthe L, Villalba-Orero M, Gómez-Salinero JM et al (2019) Severe cardiac dysfunction and death caused by arrhythmogenic right ventricular cardiomyopathy type 5 are improved by inhibition of glycogen synthase kinase-3β. Circulation 140(14):1188–1204. https://doi.org/10.1161/CIRCULATIONAHA.119.040366
55. Sharma AK, Kumar A, Taneja G et al (2018) Combined and individual strategy of exercise generated preconditioning and low dose copper nanoparticles serve as superlative approach to ameliorate ISO-induced myocardial infarction in rats. Pharmacol Rep 70(4):789–795. https://doi.org/10.1016/j.pharep.2018.02.023
56. Kamo N, Ke B, Busuttil RW, Kupiec-Weglinski JW (2013) PTEN-mediated Akt/β-catenin/Foxo1 signaling regulates innate immune responses in mouse liver ischemia/reperfusion injury. Hepatology 57(1):289–298. https://doi.org/10.1002/hep.25958
57. Ozer MK, Parlakpinar H, Cigremis Y et al (2005) Ischemia-reperfusion leads to depletion of glutathione content and augmentation of malondialdehyde production in the rat heart from overproduction of oxidants: can caffeic acid phenethyl ester (CAPE) protect the heart? Mol Cell Biochem 273(1–2):169–175
58. Chen Z, Siu B, Ho YS et al (1998) Overexpression of MnSOD protects against myocardial ischemia/reperfusion injury in transgenic mice. J Mol Cell Cardiol 30(11):2281–2289. https://doi.org/10.1006/jmcc.1998.0789
59. Bolli R (1988) Oxygen-derived free radicals and postischemic myocardial dysfunction ("stunned myocardium"). J Am Coll Cardiol 12(1):239–249. https://doi.org/10.1016/0735-1097(88)90381-6
60. Samimi F, Namiranian N, Sharifi-Rigi A et al (2024) Coenzyme Q10: a key antioxidant in the management of Diabetes-induced cardiovascular complications—an overview of mechanisms and clinical evidence. Int J Endocrinol 2024:2247748. https://doi.org/10.1155/2024/2247748
61. Chen H, Tang Y, Ren P, Wu W (2025) The unmet promise: a critical review of antioxidant strategies in myocardial ischemia-reperfusion injury and the path towards precision medicine. Front Pharmacol 16:1693441. https://doi.org/10.3389/fphar.2025.1693441
62. Younis NS, Elsewedy HS, Soliman WE et al (2021) Geraniol isolated from lemon grass to mitigate doxorubicin-induced cardiotoxicity through Nrf2 and NF-κB signaling. Chem Biol Interact 347:109599. https://doi.org/10.1016/j.cbi.2021.109599
63. King TD, Clodfelder-Miller B, Barksdale KA, Bijur GN (2008) Unregulated mitochondrial GSK3beta activity results in NADH: ubiquinone oxidoreductase deficiency. Neurotox Res 14(4):367–382. https://doi.org/10.1007/BF03033861
64. Ciotti S, Iuliano L, Cefalù S et al (2020) GSK3β is a key regulator of the ROS-dependent necrotic death induced by the quinone DMNQ. Cell Death Dis 11(1):2. https://doi.org/10.1038/s41419-019-2202-0
65. Zhang L, Cao M, Yu Z et al (2020) The restoration of Wnt/β-catenin signalling activity by a tuna backbone-derived peptide ameliorates hypoxia-induced cardiomyocyte injury. Am J Transl Res 12(9):5221–5236
66. Alghibiwi HK, Alhusiani AM, Sarawi WS et al (2025) Coenzyme Q10 and its liposomal form prevent copper cardiotoxicity by attenuating oxidative stress, TLR-4/NF-κB signaling and necroptosis in rats. Cell Mol Biol (Noisy-le-grand). 71(1):118–124. https://doi.org/10.14715/cmb/2025.70.1.13
67. Cortés-Vieyra R, Silva-García O, Gómez-García A et al (2021) Glycogen Synthase Kinase 3β modulates the inflammatory response activated by bacteria, viruses, and parasites. Front Immunol 12:675751. https://doi.org/10.3389/fimmu.2021.675751
68. Medunjanin S, Schleithoff L, Fiegehenn C et al (2016) GSK-3β controls NF-kappaB activity via IKKγ/NEMO. Sci Rep 6:38553. https://doi.org/10.1038/srep38553
69. Schwabe RF, Brenner DA (2002) Role of glycogen synthase kinase-3 in TNF-alpha-induced NF-kappaB activation and apoptosis in hepatocytes. Am J Physiol Gastrointest Liver Physiol 283(1):G204-211. https://doi.org/10.1152/ajpgi.00016.2002
70. Wang Y, Shou X, Wu Y, Li D (2024) Immuno-inflammatory pathogenesis in ischemic heart disease: perception and knowledge for neutrophil recruitment. Front Immunol 15:1411301. https://doi.org/10.3389/fimmu.2024.1411301
71. Jordan JE, Zhao Z-Q, Vinten-Johansen J (1999) The role of neutrophils in myocardial ischemia–reperfusion injury. Cardiovasc Res 43(4):860–878. https://doi.org/10.1016/S0008-6363(99)00187-X
72. Sahna E, Deniz E, Bay-Karabulut A, Burma O (2008) Melatonin protects myocardium from ischemia-reperfusion injury in hypertensive rats: role of myeloperoxidase activity. Clin Exp Hypertens 30(7):673–681. https://doi.org/10.1080/10641960802251966
73. de Carvalho KIM, Bonamin F, Dos Santos RC et al (2014) Geraniol-a flavoring agent with multifunctional effects in protecting the gastric and duodenal mucosa. Naunyn Schmiedebergs Arch Pharmacol 387(4):355–365. https://doi.org/10.1007/s00210-013-0947-z
74. Mohseni M, Vafa M, Zarrati M et al (2015) Beneficial effects of Coenzyme Q10 supplementation on lipid profile and Interleukin-6 and Intercellular Adhesion Molecule-1 reduction, preliminary results of a double-blind trial in acute myocardial infarction. Int J Prev Med 6:73. https://doi.org/10.4103/2008-7802.162461
75. Litt MR, Jeremy RW, Weisman HF et al (1989) Neutrophil depletion limited to reperfusion reduces myocardial infarct size after 90 minutes of ischemia. Evidence for neutrophil-mediated reperfusion injury. Circulation 80(6):1816–1827
76. Romson JL, Hook BG, Kunkel SL et al (1983) Reduction of the extent of ischemic myocardial injury by neutrophil depletion in the dog. Circulation 67(5):1016–1023
77. Nicholls SJ, Hazen SL (2005) Myeloperoxidase and cardiovascular disease. Arterioscler Thromb Vasc Biol 25(6):1102–1111. https://doi.org/10.1161/01.ATV.0000163262.83456.6d
78. Zhao K, Chen C, Shi Q et al (2014) Inhibition of glycogen synthase kinase-3β attenuates acute kidney injury in sodium taurocholate-induced severe acute pancreatitis in rats. Mol Med Rep 10(6):3185–3192. https://doi.org/10.3892/mmr.2014.2650
79. Kajstura J, Cheng W, Sarangarajan R et al (1996) Necrotic and apoptotic myocyte cell death in the aging heart of Fischer 344 rats. Am J Physiol 271(3 Pt2):H1215-1228. https://doi.org/10.1152/ajpheart.1996.271.3.H1215
80. Chen Z, Chua CC, Ho Y-S et al (2001) Overexpression of Bcl-2 attenuates apoptosis and protects against myocardial I/R injury in transgenic mice. Am J Physiol Heart Circ Physiol 280(5):H2313–H2320
81. Astani K, Bashiri J, Pourrazi H, Nourazar MA (2022) Effect of high-intensity interval training and coenzyme Q10 supplementation on cardiac apoptosis in obese male rats. ARYA Atheroscler 18(2):1–9. https://doi.org/10.48305/arya.v18i0.2459
82. Murphy E, Steenbergen C (2008) Mechanisms underlying acute protection from cardiac ischemia-reperfusion injury. Physiol Rev 88(2):581–609. https://doi.org/10.1152/physrev.00024.2007

Publisher's Note